Investigating the Effect of Bacteriophages on Bacterial FtsZ Localisation

Gurneet K. Dhanoa[1], Inbar Kushnir[1], Udi Qimron[2], David Roper[1], Antonia P. Sagona[1*]

[1]School of Life Sciences, Faculty of Science, University of Warwick, United Kingdom, [2]Department of Microbiology and Clinical Immunology, Sackler Faculty of Medicine, Tel Aviv University, Israel

Submitted to Journal:
Frontiers in Cellular and Infection Microbiology

Specialty Section:
Microbiome in Health and Disease

Article type:
Original Research Article

Manuscript ID:
863712

Received on:
27 Jan 2022

Revised on:
03 Jul 2022

Journal website link:
www.frontiersin.org

Conflict of interest statement

The authors declare that the research was conducted in the absence of any commercial or financial relationships that could be construed as a potential conflict of interest

Author contribution statement

G.K.D designed and performed experiments, wrote and revised the manuscript. I.K. performed experiments. U.Q. revised the manuscript. D.I.R. advised on experimental design and set up and revised the manuscript. A.P.S conceived the idea, designed experiments, supervised the study and revised the manuscript. All the authors approved the manuscript.

Keywords

Bacteriophages, ftsZ, Microscopy, inhibitors, filamentation, Human cells

Abstract

Word count: 248

Escherichia coli is one of the most common Gram-negative pathogens and is responsible for infection leading to neonatal meningitis and sepsis. The FtsZ protein is a bacterial tubulin homolog required for cell division in most species, including E. coli. Several agents that block cell division have been shown to mislocalise FtsZ, including the bacteriophage T7 -encoded Kil peptide, resulting in defective cell division and a filamentous phenotype, making FtsZ an attractive target for antimicrobials. In this study we have used an in vitro meningitis model system for studying the effect of bacteriophages on FtsZ using fluorescent E. coli EV36/FtsZ-mCherry and K12/FtsZ-mNeon strains. We show localisation of FtsZ to the bacterial cell midbody as a single ring during normal growth conditions, and mislocalisation of FtsZ producing filamentous multi-ringed bacterial cells upon addition of the known inhibitor Kil peptide. We also show that when bacteriophages K1F-GFP and T7-mCherry were applied to their respective host strains, these phages can inhibit FtsZ and block bacterial cell division leading to a filamentous multi-ringed phenotype, potentially delaying lysis and increasing progeny number. This occurs in the exponential growth phase, as actively dividing hosts are needed. We present that the ZapA protein is needed for phage inhibition by showing a phenotype recovery with a ZapA mutant strain, and we show that the FtsI protein is also mislocalised upon phage infection. Finally, we show that the T7 peptide gp0.4 is responsible for inhibition of FtsZ in K12 strains by observing a phenotype recovery with a T7Δ0.4 mutant.

Contribution to the field

Antimicrobial resistance is a growing problem worldwide and has created a need for novel antibacterial agents and strategies. Bacteriophages are viruses that infect bacteria and provide a potential solution to this problem, and we wish to study the mechanisms that bacteriophages use to target their host bacteria. FtsZ is a protein necessary for bacterial cell division and we investigate how E. coli FtsZ localisation is affected upon bacteriophage application. We show that different phages and their peptides, such as Kil peptide, T7 bacteriophage and K1F bacteriophage, can inhibit the bacterial FtsZ protein to block host cell division by creating long filamentous cells containing multiple Z-rings. We further show the potential mechanism of this process in the case of T7 bacteriophage. Our results provide the basis for better understanding how bacteriophages act towards their host, and how FtsZ can be used as a potential target and biomarker for novel antimicrobials.

Ethics statements

Studies involving animal subjects

Generated Statement: No animal studies are presented in this manuscript.

Studies involving human subjects

Generated Statement: No human studies are presented in this manuscript.

Inclusion of identifiable human data

Generated Statement: No potentially identifiable human images or data is presented in this study.

Data availability statement

Generated Statement: The original contributions presented in the study are included in the article/supplementary material, further inquiries can be directed to the corresponding author/s.

Investigating the Effect of Bacteriophages on Bacterial FtsZ Localisation

Gurneet K. Dhanoa[1], Inbar Kushnir[1], Udi Qimron[2], David I. Roper[1] and Antonia P. Sagona[1*]

1 School of Life Sciences, University of Warwick, Gibbet Hill Road, Coventry, CV4 7AL, UK

2 Department of Clinical Microbiology and Immunology, Sackler School of Medicine, Tel Aviv University, Tel Aviv 69978, Israel

*Corresponding author: A.Sagona@warwick.ac.uk

Contribution to Field

Antimicrobial resistance is a growing problem worldwide and has created a need for novel antibacterial agents and strategies. Bacteriophages are viruses that infect bacteria and provide a potential solution to this problem, and we wish to study the mechanisms that bacteriophages use to target their host bacteria. FtsZ is a protein necessary for bacterial cell division and we investigate how *E. coli* FtsZ localisation is affected upon bacteriophage application. We show that different phages and their peptides, such as Kil peptide, T7 bacteriophage and K1F bacteriophage, can inhibit the bacterial FtsZ protein to block host cell division by creating long filamentous cells containing multiple Z-rings. We further show the potential mechanism of this process in the case of T7 bacteriophage. Our results provide the basis for better understanding how bacteriophages act towards their host, and how FtsZ can be used as a potential target and biomarker for antimicrobials.

Abstract

Escherichia coli is one of the most common Gram-negative pathogens and is responsible for infection leading to neonatal meningitis and sepsis. The FtsZ protein is a bacterial tubulin homolog required for cell division in most species, including *E. coli*. Several agents that block cell division have been shown to mislocalise FtsZ, including the bacteriophage λ-encoded Kil peptide, resulting in defective cell division and a filamentous phenotype, making FtsZ an attractive target for antimicrobials. In this study we have used an *in vitro* meningitis model system for studying the effect of bacteriophages on FtsZ using fluorescent *E. coli* EV36/FtsZ-mCherry and K12/FtsZ-mNeon strains. We show localisation of FtsZ to the bacterial cell midbody as a single ring during normal growth conditions, and mislocalisation of FtsZ producing filamentous multi-ringed bacterial cells upon addition of the known inhibitor Kil peptide. We also show that when bacteriophages K1F-GFP and T7-mCherry were applied to their respective host strains, these phages can inhibit FtsZ and block bacterial cell division leading to a filamentous multi-ringed phenotype, potentially delaying lysis and increasing progeny number. This occurs in the exponential growth phase, as actively dividing hosts are needed. We present that the ZapA protein is needed for phage inhibition by showing a phenotype recovery with a ZapA mutant strain, and we show that the FtsI protein is also mislocalised upon phage infection. Finally, we show that the T7 peptide gp0.4 is responsible for inhibition of FtsZ in K12 strains by observing a phenotype recovery with a T7Δ0.4 mutant.

Introduction

Antimicrobial resistance is a growing problem worldwide and infections caused by Gram-negative bacteria are particularly concerning, as these organisms are highly efficient at acquiring genes for antibiotic drug resistance[1,2], in addition to permeability issues presented by the outer membrane. This has led to the need for novel antibacterial agents and model systems in which to test them. A potential target for new molecules could be the bacterial cell division machinery as this is essential for bacterial propagation and survival and is directly related to bacterial cell wall biosynthesis which is a validated target for natural product and semisynthetic clinically used antibiotics[3].

Escherichia coli is one of the most common Gram-negative pathogens and is responsible for many different diseases. For example, *E. coli* O18:K1:H7 is responsible for secondary infections in burn patients, neonatal meningitis[4] and sepsis, which can rapidly lead to shock and mortality[5]. Around 80% of the *E. coli* strains that are able to cause meningitis are of the K1 capsule type[6]. The K1 antigen produced by these strains makes up a thick polysaccharide capsule, which aids pathogenicity by immune system evasion, giving bacterial cells the ability to cross certain barriers (such as the blood brain barrier) and defends against certain bacteriophages[7].

Bacteriophages (phages) are viruses that infect bacteria. Their potential to kill bacteria was first discovered in 1917[8], but despite their undaunted therapeutic potential they were widely disregarded as therapeutic agents in Western nations due to the discovery of small molecule antibiotics[9]. However, the worldwide rise of multi-drug resistant bacteria has led to reinvestigation of phage therapy as an alternative to antibiotics in human and animal infections. T7 is a small bacteriophage with a genome of ~40 kbp encapsulated in a 55 nm icosahedral head[10], which infects *E. coli* and related enteric bacteria, encoding a tail fibre that specifically binds to lipopolysaccharide and recognises many *E. coli* K12 strains[11]. Laboratory strains of K12 are similar to and share many genes and phenotypes with pathogenic strains, for example *E. coli* O157:H7, so inhibitors of these strains are also likely effective against pathogens[12-14]. The K1F phage is a natural T7-like phage which infects *E. coli* O18:K1:H7. It is similar to T7 at the genome scale, although rather than the T7 tail fibre protein it incorporates the endosialidase enzyme into its tail structure, allowing attachment to and degradation of the K1 polysaccharide capsule of its host[7].

The bacterial filamentous temperature sensitive Z (FtsZ) protein is a tubulin homolog required for cell division in most species, including *E. coli*[15]. It is comprised of a globular domain, made up of two subdomains, which can fold independently[16]. FtsZ monomers in the cytoplasm undergo GTP-dependent polymerisation into single stranded protofilaments, which bundle together through lateral interactions[17]. FtsZ polymerises to assemble a ring structure (called the Z-ring) at the division site, which recruits other cell division components, such as FtsI and ZapA[18], ready to initiate cytokinesis[15]. Since FtsZ is the first protein in the divisome and is needed for downstream recruitment, it would make a good target for novel antibiotics[3,19], specifically aiming to inhibit FtsZ polymerisation[20]. Changes in the polymerisation of FtsZ or GTPase activity would prevent formation of the Z-ring and septum formation, which would in turn block cell division and cause cell death, making FtsZ a potential target for new antibacterial agents, as demonstrated by the mode of action of PC1900723[21]. The Kil peptide of bacteriophage λ prevents FtsZ polymerisation and therefore Z-ring formation, leading to filamentation of *E. coli* cells and cell death[17]. Kil has been shown to block FtsZ from forming protofilaments during the lytic cycle, and it has been suggested that Kil can directly interact with FtsZ *in vitro* for ZipA-dependant inhibition of the Z-ring[17]. At high concentrations Kil may be able to sequester FtsZ subunits and reduces their GTPase activity[22]. The gene product (gp) 0.4 protein expressed by bacteriophage T7 prevents FtsZ assembly to give elongated bacterial cells, thereby enhancing T7's competitiveness[23]. Gp0.4 is a non-essential gene transcribed around 2 min after infection with the early genes[24]. It has previously been shown that purified FtsZ is inhibited by purified gp0.4 to block Z-ring assembly *in vitro*, along with *in vivo* studies which found that gp0.4 specifically binds to and interacts with FtsZ[23].

Several features of FtsZ make it an attractive drug target: it performs an essential set of functions in the majority of bacterial pathogens[19], it has a specific role in prokaryotic cell division related to cell wall biosynthesis which is a proven target for antimicrobial agents, it is conserved across the vast majority of bacterial and archaeal species[15] and it is absent in human and animals so should not exhibit adverse effects on host cells[25].

The aim of this study was to investigate the effect of bacteriophages and their peptides on the localisation of FtsZ during infection. We used a previously developed *in vitro* meningitis model system[26] to study the effect of bacteriophages on FtsZ using fluorescent *E. coli* EV36/FtsZ-mCherry[27,28] and K12/FtsZ-mNeon[16] strains in

the hCMEC human brain cell line. We investigate FtsZ localisation in both intracellular and extracellular bacteria within a human cell environment, in order to understand better the cell biology mechanisms during phage therapy. We show localisation of FtsZ to the bacterial cell midbody as a single ring during normal growth conditions in the absence and presence of human cells and mislocalisation of FtsZ to give filamentous multi-ringed cells upon addition of the known inhibitor Kil peptide[17]. We show that bacteriophages K1F-GFP[29] and T7-mCherry are able to inhibit FtsZ and block bacterial cell division in the exponential growth phase only, since an actively dividing host is needed. We show that inhibition of the divisome proteins FtsI and ZapA occurs, and potentially the inhibition of MinC. Finally, we show that the T7 peptide gp0.4 is responsible for inhibition of FtsZ in K12 strains by observing a phenotype recovery with a T7Δ0.4 mutant[23], and this peptide potentially acts to delay host cell lysis and increase phage progeny numbers.

Materials and Methods

Human cell culture

The human cerebral microvascular endothelial cell (hCMEC) line (Merck, UK) was cultured in EndoGRO-MV Complete Media (Merck) supplemented with 1% penicillin-streptomycin and grown at 37°C with 5% CO_2 in culture vessels coated with 5 µg/cm^2 Collagen Type 1 (Merck). Prior to an experiment, the cells were seeded onto coverslips in a 6-well plate or a fluorodisc in culture media at a density of 4×10^4 cells/ml and left for 24 hours to settle. The culture media was then replaced with Leibovitz L-15 media (Lonza) and the cells were moved to a 37°C incubator suitable for bacterial infection.

Bacterial cultures

Bacterial cultures were grown from a single colony in lysogeny broth (LB), supplemented with the appropriate antibiotic if needed, and grown in a 37°C shaking incubator. The seven bacterial strains used in this study are listed in Table 1. During experiments bacterial cells were added during the exponential growth phase at OD_{600} 0.3 (unless otherwise stated as stationary) and incubated for one hour prior to fixation or phage addition.

Strain	Description	Source
Escherichia coli EV36	*E. coli* K1/K12 hybrid suitable for Class 1 laboratory work while maintaining phenotypic properties of a pathogenic K1 strain	Dr Eric R. Virm[28]
Escherichia coli EV36/FtsZmCherry	Derivative of EV36 transformed with a pBAD30FtsZ-mCherry plasmid and cultured under 35 µg/ml chloramphenicol selection	Plasmid kindly provided by Dr Kenn Gerdes[27], transformed in this study
Escherichia coli EV36/Kil	Derivative of EV36 transformed with a pBAD33-Kil plasmid and cultured under 35 µg/ml chloramphenicol selection	Plasmid kindly provided by Dr William Margolin[17], transformed in this study
Escherichia coli K12 FtsZ-mNeon	*E. coli* BW27783 strain which has had its wild type *ftsZ* gene replaced with FtsZ-mNeonGreen	Dr Harold Erickson[30]
Escherichia coli K12/FtsZmNeon/Kil	Derivative of K12/FtsZ-mNeon transformed with a pBAD33-Kil peptide plasmid and cultured under 35 µg/ml chloramphenicol selection	Plasmid kindly provided by Dr William Margolin[17], transformed in this study

Escherichia coli K12ΔzapA	*E. coli* BW25113 K12 strain from the Keio collection with a deleted *zapA* gene that has been replaced by a kanamycin resistance cassette. Cultured under 50 µg/ml kanamycin selection	OEC4987-200828117, Keio collection[31]
Escherichia coli K12ΔminC	*E. coli* BW25113 K12 strain from the Keio collection with a deleted *minC* gene that has been replaced by a kanamycin resistance cassette. Cultured under 50 µg/ml kanamycin selection	OEC4987-213605848, Keio collection[31]

Table 1: Bacterial strains used in this study

Bacteriophage propagation and purification

The bacteriophages used in this study are listed in Table 2. *E. coli* EV36 was used as a host to grow and purify K1F-GFP phage and K12/FtsZ-mNeon was used as a host to grow and purify T7 phage, T7-mCherry phage and T7Δ0.4 phage. After host clearance each phage propagation culture was centrifuged at 3220 x g for 15 minutes. The resulting supernatant was filter sterilised and incubated on ice with 0.2 M NaCl for 1 hour, then centrifuged at 3220 x g for 15 minutes at 4°C. The supernatant was then incubated with 10% w/v PEG8000 overnight at 4°C to precipitate the phage, and then centrifuged at 3220 x g for 15 minutes at 4°C. The resulting phage pellet was resuspended in a SM

buffer 1 (1 M NaCl, 8 mM $MgSO_4 \cdot 7H_2O$, 25 mM Tris-HCl). A CsCl density gradient was set up with three solutions of densities 1.7, 1.5 and 1.4 g/ml, along with phage solution with CsCl added to give a density of 1.3 g/ml. The solutions were added in equal volumes to a centrifuge tube, starting with the heaviest, and centrifuged at 125,000x g for 20 hours at 4°C. The resulting phage band was extracted and placed in dialysis tubing (MWCO of 14kDa) and dialysed overnight in SM buffer 1 at 4°C, followed by dialysis in SM buffer 2 (100 mM NaCl, 8 mM $MgSO_4 \cdot 7H_2O$, 25 mM Tris-HCl) for 2 hours at room temperature twice. After dialysis the purified phage was retrieved and stored at -20°C, and the phage titre was found by plaque assay. WT T7, T7-mCherry and K1F-GFP phage stocks were diluted to approximately 10^9 pfu/ml for use in experiments. For experiments phages were incubated for one hour prior to fixation.

Phage	**Description**	**Source**
K1F-GFP	A K1F phage derivative engineered to express GPF which shows a high specificity towards K1 capsule bacteria.	K1F from Dr Dean Scholl[7], K1F-GFP from Dr Antonia Sagona [29]
T7	Extensively used strain showing high specificity to commensal *E. coli* K12 strains.	Dr Ian Molineux, Texas USA [32]
T7-mCherry	A T7 phage derivative engineered with genomic integration of mCherry, showing high specificity to commensal *E. coli* K12 strains.	This study
T7Δ0.4	T7 phage derivative engineered with a knockout of gp0.4 showing high specificity towards commensal *E. coli* K12	Dr Udi Qimron[23]

Table 2: Phage strains used in this study

Engineering of T7-mCherry phage

Plasmid construction – the pSB1C3 plasmid (Registry of Standard Biological Parts http://parts.igem.org/Main_Page) contained chloramphenicol resistance. The synthetic gBlock was ordered from Integrated DNA Technologies, with EcoRI and SpeI sites to ligate to the corresponding restriction sites of the pSB1C3 plasmid. The gBlock (Fig S1) was designed to contain the mCherry gene[33] flanked by 150bp homology regions of the C-terminus (excluding the stop codon) of the T7 minor capsid protein (gene 10), along with a linker sequence. A PCR was performed to amplify the insert using primers AG005 and AG006 (Table S1). The insert and vector were digested with restriction enzymes at 37°C for 1 hour, purified using a GeneJET PCR Purification Kit (ThermoFisher Scientific) and then ligated (150 ng insert and 50 ng vector) with DNA T4 ligase overnight at 4°C.

Sequencing the plasmid – after ligation the resulting vector was transformed into electrocompetent K12 cells, plated on chloramphenicol agar overnight, and plasmid was miniprepped from the colonies using a QIAprep Spin kit. The miniprepped DNA was sent for Sanger sequencing by GATC using the AG005 primer. One plasmid returned a matching sequence and was used for engineering the phage.

Homologous recombination - wild type T7 phages were propagated with electrocompetent K12/FtsZmNeon transformed with the donor plasmid at a low OD_{600} of 0.2. Homologous recombination occurred between the homology regions of the plasmid and genome of some phages, resulting in a mixed population lysate which was centrifuged at 3220 x g for 15 minutes and then filter sterilised.

Screening for engineered phage – the presence of engineered phage was found by PCR analysis of the lysate using the primers mCherry-forward and mCherry-rev (Table S1). Positive lysate was then plated out on host lawn at an appropriate dilution to give individual phage plaques. 10 plaques were chosen and used as a template for a second PCR screen. The plaques showing positive bands were propagated as before and the lysate was plated for a second plaque assay, and plaques were again checked by a PCR screen. Positive phage was propagated, CsCl purified and further checked for mCherry fluorescence by confocal and electron microscopy.

Bacterial and phage infections of human cells

Cultures of hCMECs were incubated with the relevant bacterial strain at OD_{600} of 0.2-0.4 which were added to the Leibovitz media for 60 minutes (unless otherwise stated) along with antibiotics or plasmid induction if needed, and if phages were being used then the phage was added at 1×10^7 pfu/ml and incubated for a further 60 minutes. Control cultures were incubated with bacteria or phage alone for 60 minutes in parallel.

To investigate if strains acted intracellularly, hCMEC cultures were infected with bacterial cultures at OD_{600} 0.3 for one hour, then incubated with 100 ug/ml gentamicin for a further two hours to kill extracellular bacteria, performed in triplicate for each condition. For each condition, a minimum of 300 human cells were counted to calculate the internalised bacteria percentages.

To quantify human cell death after bacterial infection, hCMEC cultures were infected with bacterial cultures at OD_{600} 0.3 for one hour, in triplicate conditions. For each condition, a minimum of 500 human cells were counted.

Immunofluorescent confocal microscopy

After bacterial and/or phage infection, hCMEC cultures were fixed with 4% paraformaldehyde (ThermoFisher Scientific) in phosphate buffered saline (PBS) for 15 minutes and then washed in PBS. Cells were then permeabilised in ice cold PEM/0.05% saponin for 5 minutes, washed, incubated with 50 mM NH_4Cl in PBS for

15 minutes, and then washed in PBS/0.05% saponin. The fixed cells were stained overnight at 4°C with anti-Prokaryotic Cell Division GTPase (FtsZ) antibody (Agrisera, Sweden) or Rabbit anti-*Escherichia coli* (strain K12) FtsI Polyclonal antibody if no fluorescent proteins were present and FtsZ or FtsI staining was needed, diluted 1:100 in 0.05% saponin in PBS. This was followed by conjugation with secondary Donkey Anti-Rabbit IgG H&L (Alexa Fluor® 488) diluted 1:500 in 0.05% saponin in PBS at room temperature for 45 minutes. For samples with fluorescent proteins, the fixed cells were stained with the following antibodies diluted in PBS/0.05% saponin for 60 minutes at room temperature: 5 µg/ml GFP-booster (Chromotek), 5 µg/ml RFP-booster (Chromotek) and 5 µg/ml Phalloidin CF680R Conjugate (Biotium).

After staining the coverslips were washed and mounted on slides with DAPI-containing Fluoroshield Mounting Medium (Abcam) and sealed. The slides were then imaged using a Zeiss LSM800 confocal microscope using the following excitation wavelengths: DAPI at 405 nm, GFP/mNeon at 488 nm, mCherry at 561 nm and phalloidin at 633 nm.

Quantification was performed by manually counting Z-rings of 75 bacterial cells per condition and measuring cell length using the Fiji (ImageJ) software for phage filamentation experiments. Data was plotted with error bars showing one standard deviation of uncertainty. For significant difference comparisons, Tukey's tests were performed and the calculated probability values (p-values) are displayed as $p < 0.05$ (*), $p < 0.01$ (**) and not statistically significant $p > 0.05$ (ns).

Live cell imaging

Cultures of bacteria alone expressing fluorescent proteins were imaged live on 2% agarose pads. Cultures of K12/FtsZ-mNeon were grown to OD_{600} 0.5 and imaged immediately. For EV36/FtsZ-mCherry, cultures were grown to OD_{600} 0.3 and induced with 0.2% arabinose for 5 minutes (stopped using 0.2% glucose) and incubated for 45 minutes to allow time for protein folding before imaging. Agarose pads were made by dissolving 0.2 g agar into 10 ml sterile water by heating, and a drop was placed onto a glass microscope slide and left to dry. 10 µl of culture was then placed onto the agarose layer and covered with a coverslip once dry. Cells were imaged using the Zeiss LSM 880 confocal microscope, with mNeon excitation at 488 nm and mCherry at 561 nm wavelengths, and transmitted light was used to visualise the cell outline.

Correlative Light and Electron microscopy

T7-mCherry phage was added to a K12/FtsZ-mNeon culture (OD_{600} 0.3) and incubated at 37°C with shaking for 60 minutes. 300 mesh copper grids (FC300Cu) were hydrophilised by glow discharge. Sample was added to the grid and incubated for 2 minutes, then 2% uranyl acetate was dropped into the grid and incubated for 2 minutes. A wash step was performed three times and blotted. 0.1% trehalose was added to the grid and incubated for 2 minutes. This was left to airdry. The sample was imaged using Zeiss LSM 880 confocal microscope (565 nm for T7-mCherry and 488 nm for K12/FtsZ-mNeon) and Jeol 2100 transmission electron microscope, overlayed using ImageJ.

Results

Visualisation of the FtsZ ring and Kil peptide-mediated inhibition of FtsZ

We firstly sought to observe Z-rings in bacterial cells, using the *E. coli* K12/FtsZ-mNeon[16] strain which has its genomic copy of the FtsZ gene replaced with FtsZ-mNeon. A crucial aspect of the design of this FtsZ construct is that the mNeon protein has been placed on an internal loop of FtsZ so that the head-to-tail mode of polymerisation required for function is not impaired[16] and the mNeon proteins are prevented from forming aggregates with each other. The Z-rings were visualised by placing exponential-phase bacterial cultures onto

2% agarose pads for visualisation by confocal microscopy. FtsZ-mNeon assembled at the cell midbody as a single Z-ring (Fig. S2A). This visualisation was repeated in the *E. coli* K1/K12 hybrid strain EV36[28], by transforming it with an arabinose-inducible FtsZ-mCherry plasmid[27] and FtsZ-mCherry forms a Z-ring at the EV36 midbody (Fig. S2B).

We next observed the phenotype of the Z-rings in a meningitis infection model, to see if FtsZ localisation changed during bacterial infection of human cells. hCMEC brain cells were infected with K12/FtsZ-mNeon culture for an hour, fixed and stained before visualising by confocal microscopy. During human cell infection FtsZ rings were still visible at the midbody of K12 cells as a single ring per cell (Fig. 1A), suggesting cells can divide normally, and this was also found for the EV36/FtsZ-mCherry strain (Fig. 1B). These data confirm that FtsZ assembles as a single ring at the cell midbody under normal bacterial growth conditions and during bacterial infection of human cells. The EV36 strain has previously been shown to have an infection rate of 20-50%, depending on the human cell line[26,29]. Since the K12 strain is non-pathogenic and not expected to act intracellularly[34,35], an internalisation experiment was done using gentamicin to kill extracellular bacteria to confirm if K12 would be present inside of human cells. This showed that only 4.1% of hCMECs infected with K12/FtsZ-mNeon had intracellular bacteria. Since the infection rate is low, for the following experiments we chose to focus on both intracellular and extracellular bacteria in the infection model for both strains. Nevertheless, both extracellular and intracellular bacteria are toxic to the human cells and have a variety of mechanisms to cause disease[36]. We confirm this by quantifying human cell death by confocal microscopy after bacterial infection of human cells and found that 5.3% of human cells died after infection with the K12 strain, and 12.1% of human cells died after infection with the EV36 strain (Figure S3). Recent studies have presented efficiency of bacteriophages in targeting both intracellular and extracellular bacteria in human cell environment[37] and bacteriophages have been shown to be more efficient in the presence of human cells[38]. It is therefore necessary to test the proposed system in infection human cells models, in order to understand better the interplay of phage and bacteria in the presence of human cells.

We then applied the known FtsZ inhibitor Kil peptide to the model system to investigate how FtsZ inhibition would appear in these conditions. Kil stops FtsZ from polymerising leading to filamentation of cells which are unable to divide, so a Kil peptide plasmid[17] was transformed into both strains. For these experiments the plasmid was induced with 0.2% arabinose for two hours. Imaging in Fig. S4A confirmed that induction of Kil in K12/FtsZ-mNeon resulted in long filamentous cells, with varying FtsZ phenotypes that ranged from distinct multiple rings (42.2% of cells) to diffuse FtsZ spread (30.1%) and cells in an intermediate phenotype (27.7%) of faint rings within a diffuse background. Previous studies have shown a diffuse FtsZ spread upon Kil inhibition using antibody staining[17], which was confirmed in Fig. S5, however, here we present that when using a fluorescent protein stably expressed, multiple distinct Z-rings still form along the cell body, potentially due to Kil not having fully acted on these cells yet.

To support these findings, images for the induction of Kil were quantified in K12/FtsZ-mNeon under the following conditions: control (no Kil induction), 1 hour induction, and 2 hour induction. The averages (Fig. S4C and S4D) showed an increase in number of Z-rings and cell length after 1 hour of Kil induction, with a further increase after 2 hours, confirming the cells are not dividing and continually elongating in the presence of Kil and formation of multiple Z rings suggests cell division had been unsuccessfully attempted. The increase seen after 2 hours compared to 1 hour suggests that the effect and phenotypes seen may be dependent on the amount of Kil peptide present in the cell.

These data support previous findings that the phage λ Kil peptide causes filamentation of *E. coli* cells by blocking cell division with diffuse FtsZ spread by antibody staining as FtsZ is unable to polymerise to form rings and further show that multiple Z-rings can form along the body of the filamentous cell as it fails to divide at new division sites when using fluorescent proteins.

Genetic engineering of a T7-mCherry phage

The K1F-GFP phage[29] has been previously engineered to express GFP, and this was first visualised in human cells vacuoles (Fig. 2A) to confirm fluorescence compared to no-phage controls as a visual control for use in confocal experiments. In order to visualise T7 phage in the K12/FtsZ-mNeon model system, we attached a fluorescent protein to the C-terminal of the phage's minor capsid protein so that it is displayed at the surface, using homologous recombination from an engineered plasmid. Presence of the mCherry gene in the phage lysate was confirmed by PCR screening of the recombinant phage genome using the primers in Table S1 and associated plaque assays (Fig. S6A-D), prior to purification of positive lysate by caesium chloride gradient purification (Fig. S6E-F). Fluorescence of the mCherry tag was further tested by confocal microscopy (Fig. 2B) showing mCherry fluorescence inside human cells after phage infection, alongside no-phage controls (Fig. S7) performed to show the fluorescence seen was from the phage label, confirming successful engineering of the T7-mCherry phagemid which was able to be taken up by human cells.

T7 phage blocks cell division in K12 by FtsZ inhibition

K1F-GFP phage was confirmed to target the EV36/FtsZ-mCherry strain (Fig. S8A), and T7-mCherry phage targets the K12/FtsZ-mNeon strain (Fig. S8B) using growth curves. This was further confirmed by correlative light and electron microscopy (CLEM) showing the formation of a septum at the midbody of cells, as well as colocalisation of FtsZ-mNeon and T7-mCherry signals within K12 cells (Fig. S9) confirming specificity of the phage.

Next the effect of T7-mCherry on FtsZ was examined by infecting hCMEC with K12/FtsZ-mNeon, followed incubation with T7-mCherry. Confocal microscopy showed that T7 phage infection caused a change from the single midbody ring previously seen and led to the formation of filamentous, multi Z-ring *E. coli* cells (Fig. 3A and 3B) which were unable to divide, suggesting T7 phage can block cell division. We were then interested to see how the Z-rings and cell length of *E. coli* changed over time in control conditions (no phage) and in the presence of T7 phage using a time series experiment. For the control, hCMECs were infected with exponential K12/FtsZ-mNeon and fixed at 15 minute intervals for 2 hours (Fig. S10). For the phage time series, hCMECs were infected with K12/FtsZ-mNeon for one hour, then T7 phage was added (Fig. S11). For each condition bacterial cells were quantified using confocal microscopy (Fig. 3C and 3D). Since K12/FtsZ-mNeon cells were incubated prior to phage addition, this meant phage time 0 minutes was equivalent to control 60 minutes so these were plotted to overlap. Larger error bars were due to the variation in phenotypes, as some cells were fully filamentous whereas others were yet to be infected. In the first 60 minutes of the control series, each cell averages one Z ring at the midbody as seen earlier in Figure 1, but later we unexpectedly see 2 polar rings in the majority of cells. Upon phage addition the number of Z-rings start to increase after 15-30 minutes, and after one hour they reach an average of 4 rings, double compared to the control. After an hour of incubation with phage there is a notable increase in cell length showing filamentation, but interestingly this does not start until about 30-45 minutes after infection, suggesting the number of rings start to increase first and then filamentation follows.

To investigate the cause of the filamentation confocal microscopy was performed using a K12ΔminC strain from the Keio collection with the *minC* gene knocked out, alongside a K12 control. Cultures were incubated for 2 hours in no-phage conditions and then stained with an FtsZ antibody and imaged (Fig. S12). The images were quantified and average cell length was plotted (Fig. 3E), showing a significant increase in cell length of K12ΔminC compared to the control, suggesting that inhibition of MinC could be causing the filamentation seen upon phage infection of cells.

Taken together these data confirm the specificity of engineered T7-mCherry for K12 strains and show that during infection the phage causes a filamentous (potentially due to MinC inhibition) non-dividing phenotype with multiple Z-rings formed where division had been attempted, similar to what was seen with the known FtsZ inhibitor Kil, suggesting that T7 phage can inhibit FtsZ to block division.

K1F phage blocks cell division in EV36 K1 by FtsZ inhibition

To investigate the effect of K1F-GFP phage on FtsZ localisation, hCMECs were infected with host EV36/FtsZ-mCherry and K1F-GFP phage. The EV36/FtsZ-mCherry cells showed a long filamentous phenotype with multiple Z-rings and DNA along the cell after K1F-GFP infection (Fig. 4A and 4B), unlike control samples, suggesting that the K1F phage can also inhibit FtsZ to block host cell division.
To further confirm this, bacterial cells were quantified for control conditions and K1F infected conditions (Fig. 4C and 4D). The control showed an average of 1.027 rings per cell as expected and after K1F-GFP infection this increases to 4.120 rings per cell, suggesting cells had attempted to divide 2-3 times unsuccessfully. There was an increase in average cell length showing cells were starting to elongate to confirm filamentation. These data shows that similarly to phages λ and T7, the K1F phage is able to inhibit FtsZ to block host cell division.

Effects of T7 bacteriophage on ZapA and FtsI divisome proteins

We hypothesised that the observed effect of FtsZ inhibition by phages may not be specific to just FtsZ and that other divisome proteins may be involved in the infection process. To test this a K12ΔzapA strain from the Keio collection with the *zapA* gene knocked out was used, alongside a K12 control. Cultures were incubated for 1 hour and then infected with T7 phage for a further hour, alongside a no phage control, and imaged by light microscopy to observe cell filamentation (Fig. 5A). The images were quantified and average cell lengths for the conditions were plotted (Fig. 5B). As previously shown there was an increase in cell length upon T7 phage infection of K12 cells as they became filamentous, but this phenotype appears to be absent during T7 phage infection of K12ΔzapA cells, suggesting that ZapA is essential for cell filamentation and the phenotype seen during phage inhibition of cell division.

Next the localisation of the FtsI protein in this system was investigated. Cultures of K12 were grown for one hour and infected with T7 phage, alongside a no-phage control, and stained with an FtsI antibody. Under normal growth conditions in the no-phage control, we see that FtsI is localising to the midbody of the cell as a single ring (Fig. 5C) as expected after recruitment by FtsZ as the divisome forms. After T7 phage infection of K12, we observe mislocalisation of FtsI (Fig. 5D). This suggests that other divisome proteins are mislocalised upon phage infection as cell division is inhibited, potentially being recruited by mislocalised FtsZ.

T7 Gp0.4 targets FtsZ to increase titres and delays lysis

It has been previously shown by light microscopy that the T7 phage peptide gp0.4 directly inhibits FtsZ and causes host cell filamentation[23] and in this study we confirm this observation by confocal microscopy, to allow visualisation of the Z-rings in the human cell model after infection with a T7Δ0.4 mutant phage[23]. hCMEC cells were treated with K12/FtsZ-mNeon followed by infection with T7mCherry or T7Δ0.4 phage, along with a control. Cells were imaged to see the resulting phenotypes (Fig. 6A-C) and for each condition was quantified and averages were plotted (Fig. 6D and 6E). Upon T7Δ0.4 addition, unlike the WT T7, the mutant-infected *E. coli* showed recovery back to a phenotype similar to the control, confirming that T7's gp0.4 targets FtsZ and

causes filamentation of the cells as well as multiple Z rings along the cell body. After 2 hours the control sample had an average of 1.920 rings per cell with an average length of 3.426 µm, and for the WT T7 infected cells this nearly doubled to an average of 3.827 rings and 6.143 µm length. Infection with T7Δ0.4 resulted in cells averaging 2.200 rings with length 3.513 µm, which closely resembles control measurements and suggests the host can divide normally with the mutant, so gp0.4 plays a role in blocking cell division via FtsZ inhibition.

We then investigated why phages may have evolved these peptides, and it has been shown that WT phage progeny is higher than T7Δ0.4 progeny via PCR[23], so we further verified this by performing plaque assays to titre phage lysate grown in the presence and absence of gp0.4 (Fig. 7A). There was nearly a 10-fold decrease in titre with the T7Δ0.4 mutant, supporting previous PCR findings, suggesting gp0.4 plays a role in increasing progeny numbers, potentially by enabling the formation of long undivided cell factories. Growth curves were done to compare phage infection and cell lysis of WT T7 and T7Δ0.4 (Fig. 7B-C) and we found that T7Δ0.4 lysed host cells after 45 minutes, whereas the WT T7 took 105 minutes, suggesting that the gp0.4 peptide has a role in delaying host cell lysis by approximately 1 hour (43%).

Phage inhibition of FtsZ is limited in the stationary phase and under bacteriostatic conditions

We then wanted to apply the same phages to the model system during the stationary phase of cell growth to test the hypothesis that phage proteins need hosts that are actively dividing and producing an FtsZ target to inhibit FtsZ and block cell division. hCMEC cells were infected with K12/FtsZ-mNeon cells from overnight cultures to give cells in the stationary phase, followed by incubation with either T7-mCherry or T7Δ0.4 phage, along with a no-phage control. Bacterial cells were quantified and plotted alongside the exponential phase quantification for comparison (Fig. 8A-B).
The average number of Z-rings in the stationary phase control was 1.160, unlike the exponential control of 1.920 rings per cell, suggesting no movement of FtsZ to confirm cells are not dividing. When the phages are applied there is an increase in ring number for both phages compared to the control, but there are less rings produced compared to the exponential phase suggesting some inhibition is taking place but it is limited in the stationary phase. There is no change in length upon either phage addition in the stationary phase, so cells are unable to filament. These data are consistent with the hypothesis that T7 inhibition of bacterial cell growth requires the presence of a functional FtsZ engaged in cell division. This was further confirmed by performing growth curves with bacteriostatic concentrations of chloramphenicol (Fig. S13), which showed the phage was unable to lyse static host cells. Finally, we investigated whether the concentration of FtsZ changed in the stationary phase and upon phage infection by live cell imaging calculation of corrected total cell fluorescence (CTCF) (Fig. 8C and Fig. S14). FtsZ-mNeon imaging shows a 2.8-fold decrease in the intensity per Z-ring in the stationary phase compared to exponential. Interestingly upon phage addition to exponential culture, the average intensity per ring almost halves, potentially due to FtsZ being spread through the elongated cell.

Discussion

In this study we used an *in-vitro* meningitis model[26] to investigate the effect of phage on bacterial FtsZ localisation during treatment, using hCMEC human brain cell cultures infected with *E. coli* EV36/FtsZ-mCherry or K12/FtsZ-mNeon strains and initially observed FtsZ localising to the cell midbody as a single ring. It has been previously shown that the bacteriophage λ Kil peptide can block FtsZ polymerisation and Z-ring formation, leading to a filamentous cell phenotype as a result of cells being unable to complete division[17]. Here we confirm this phenotype and further show for the first time that Kil also leads to multiple Z-ring formation in the filamentous cell.

We have engineered a fluorescent T7-mCherry phage by homologous recombination which specifically targets K12 strains of *E. coli*. This has allowed us to observe invasion of hCMEC human brain cells by this phage and show that during T7 infection of K12, there is a mislocalisation of FtsZ into multiple rings along a filamentous cell that is unable to divide, suggesting that T7 phage inhibits FtsZ to block cell division. These multiple rings may represent attempts at cell division, where the inhibitor has stalled cytokinesis, creating multiple midbodies since the new upcoming cells are unable to separate. The filamentation seen may be due to MinC inhibition, since we show a MinC mutant strain becomes filamentous in normal growth conditions.
We have also shown that actively dividing cells are needed for phage inhibition of FtsZ, as inhibition is limited in the stationary phase. Since phage is still able to bind and infect these cells, we hypothesise that the decrease in average cell length and ring number is due to the small number of cells that are still dividing at a slower rate, leading to less of an effect seen from gp0.4 or any other inhibitor.

The T7 phage inhibition of FtsZ is likely to have a similar effect on other divisome proteins since proteins such as ZipA and FtsA have been shown to be recruited to the FtsZ ring site so it is likely they will also mislocalise away from the midbody as new Z-rings form along the cell[17,39]. Here we present that the ZapA protein is needed for phage inhibition of FtsZ by showing a phenotype recovery with a ZapA mutant strain, and we show that the FtsI protein is also mislocalised upon phage infection. We propose that this is effect is specific to the divisome due to the phenotype seen, for example if the elangosome[18] protein MreB was inhibited and mislocalised we would expect to see lemon shaped cells[40] rather than elongation, therefore these other proteins appear to be functioning as expected.

A recent study has shown that the T7 phage peptide gp0.4 directly inhibits FtsZ by binding the protein and preventing Z-ring assembly, giving *E. coli* cells an elongated phenotype under light microscopy, to enhance the phages competitive ability[23]. In this study we further investigate how and why phage proteins might target FtsZ, using the T7Δ0.4 mutant to confirm that the T7 peptide gp0.4 is responsible for inhibiting FtsZ by showing a reversal in phenotype to normal single central ring growth compared to the filamentous multi ring phenotype seen with the wild type. Plaque assays were performed to titre propagated T7Δ0.4 and wild type T7 phages and found a 10-fold decrease in titre with the mutant suggesting the gp0.4 peptide assists in increasing phage progeny, confirming what was previously shown by Kiro *et al* using PCR analysis[23], to give the phage a competitive advantage by producing more progeny per burst cycle.

Here we present for the first time that gp0.4 delays host cell lysis, showing that the mutant T7Δ0.4 phage lysed bacterial culture around 60 min before the wild type T7 containing gp0.4 lysed. The Kil peptide has similarly been reported to delay lysis by 30%[17], so it seems both these phage peptides targeting FtsZ are able to cause this delay. Lysis is initiated when cell signals such as lysins reach a certain threshold concentration towards the end of the infection cycle[41]. Here we hypothesise that the delay in lysis is due to the cell filamentation increasing the volume of the infected cell and therefore it is taking longer for a similar number of signals to reach the threshold concentration. This could also explain the reduced titre seen for the mutant, since lysis occurs faster, so the host cell bursts prematurely and the phage does not fully exploit the entire resources.

We report for the first time that the K1F phage is also able to target FtsZ and leads to a multi-ringed filamentous phenotype to block cell division, suggesting multiple phages have evolved this strategy.
K1F is a natural T7-like phage[7]. Interestingly it lacks the 0.4 gene found in T7 but still shows the same phenotype, so it has evolved another peptide with the same function which is currently unknown. Further studies on K1F phage to find this inhibitory peptide could lead to the discovery of a new antimicrobial compound. A BLAST search on the National Centre for Biotechnology Information (NCBI) database showed that the K1F phage genome had no sequence similarity to the *kil* or *gp0.4* genes, so the inhibitory peptide is likely to be novel from these.

We saw that after about 75 min into normal growth the K12 bacterial cells seem to form two polar Zrings instead of the characteristic single midbody ring in the absence of phage infection. The location of the Z-ring is restricted by regulatory systems such as Min in *E. coli*[42], so two Z-rings may demonstrate a time within the cell in which the Min system has not started to discriminate against FtsZ at the poles[43] and has also been previously shown that competition between FtsZ and the Min system could be the cause for these polar sites [43]. We further show that a knockout mutant lacking the MinC protein displays a filamentous phenotype under normal growth conditions.

In conclusion, we have shown that FtsZ assembles as a single ring at the cell midbody under normal bacterial growth conditions during infection of human cells and shown that this localisation is disrupted to give a filamentous phenotype with multiple Z-rings along the cell body via phage peptides such as Kil, Gp0.4 and an unknown K1F phage protein during phage infection. This inhibition may function to delay host lysis and increase phage progeny numbers and occurs during the exponential phase of bacterial growth when cells are dividing. This furthers our understanding of the mechanism that phages use to control their bacterial host, allowing them to be considered as future antimicrobials.

Data availability

The data generated in this study are available from the corresponding author upon reasonable request.

Acknowledgements

This work was funded by the Biotechnology and Biological Sciences Research Council (BBSRC) Future Leader Fellowship (ref. BB/N011872/1) to A.P.S. and the BBSRC and University of Warwick funded Midlands Integrative Biosciences Training Partnership (MIBTP) to G.K.D. I.K was supported by the MBio Masters programme at the University of Warwick. The authors would like to thank Dr Harold Erickson (Duke University School of Medicine) for providing the K12/FtsZ-mNeon strain, Dr Kenn Gerdes (University of Copenhagen) for providing the FtsZ-mCherry plasmid, and Dr William Margolin (University of Texas McGovern Medical School) for providing the Kil peptide plasmid. We would also like to thank Dr Ian Hands-Portman for confocal microscopy training and CLEM imaging, Dr Saskia Bakker at the Warwick Advanced Bioimaging Research Technology Platform for electron microscopy training and John Moat and Abby Henney at the Warwick Antimicrobial Screening Facility for identifying minimum inhibitory concentrations.

The authors declare no competing interests.

Author contributions

G.K.D designed and performed experiments, wrote and revised the manuscript. I.K. performed experiments. U.Q. revised the manuscript. D.I.R. advised on experimental design and set up and revised the manuscript. A.P.S conceived the idea, designed experiments, supervised the study and revised the manuscript. All the authors approved the manuscript.

References

1 Peleg, A. Y. & Hooper, D. C. Hospital-acquired infections due to gram-negative bacteria. *N Engl J Med* **362**, 1804-1813, doi:10.1056/NEJMra0904124 (2010).

2 ECDC. Annual Report of the European Antimicrobial Resistance Surveillance Network 2018. (European Centre for Disease Prevention and Control, Stockholm, 2019).

3 Araya, G. *et al.* Inhibition of Escherichia coli and Bacillus subtilis FtsZ Polymerization and Bacillus subtilis Growth by Dihydroxynaphtyl Aryl Ketones. *Front Microbiol* **10**, 1225, doi:10.3389/fmicb.2019.01225 (2019).
4 Baud, O. & Aujard, Y. Neonatal bacterial meningitis. *Handb Clin Neurol* **112**, 1109-1113, doi:10.1016/B978-0-444-52910-7.00030-1 (2013).
5 Nathan A. Busch, E. M. Z., Paul M. Loiselle, Edward A. Carter, Jennifer E. Allaire, Martin l. Yarmush, H. Shaw Warren. . A Model of Infected Burn Wounds Using Escherichia coli O18:K1:H7 for the Study of Gram-Negative Bacteremia and Sepsis. *Infection and Immunity* **68**, 3349-3351 (2000).
6 Kaper, J. B., Nataro, J. P. & Mobley, H. L. Pathogenic Escherichia coli. *Nat Rev Microbiol* **2**, 123140, doi:10.1038/nrmicro818 (2004).
7 Scholl, D. & Merril, C. The genome of bacteriophage K1F, a T7-like phage that has acquired the ability to replicate on K1 strains of Escherichia coli. *J Bacteriol* **187**, 8499-8503, doi:10.1128/JB.187.24.8499-8503.2005 (2005).
8 D'Herelle, F. On an invisible microbe antagonistic toward dysenteric bacilli: brief note by Mr. F. D'Herelle, presented by Mr. Roux. 1917. *Res Microbiol* **158**, 553-554, doi:10.1016/j.resmic.2007.07.005 (1917).
9 Martha R.J. Clokie, A. D. M., Andrey V. Letarov, Shaun Heaphy. Phages in Nature. *Bacteriophage* **1**, 31-45 (2011).
10 Xu, H. *et al.* Engineering T7 bacteriophage as a potential DNA vaccine targeting delivery vector. *Virol J* **15**, 49-49, doi:10.1186/s12985-018-0955-1 (2018).
11 Scholl, D., Adhya, S. & Merril, C. Escherichia coli K1's capsule is a barrier to bacteriophage T7. *Appl Environ Microbiol* **71**, 4872-4874, doi:10.1128/AEM.71.8.4872-4874.2005 (2005).
12 Mahata, T. *et al.* A phage mechanism for selective nicking of dUMP-containing DNA. *Proceedings of the National Academy of Sciences* **118**, e2026354118, doi:10.1073/pnas.2026354118 (2021).
13 Koli, P. *et al.* Conversion of Commensal Escherichia coli K-12 to an Invasive Form via Expression of a Mutant Histone-Like Protein. *mBio* **2**, e00182-00111, doi:10.1128/mBio.00182-11.
14 Browning, D. F. *et al.* Laboratory adapted Escherichia coli K-12 becomes a pathogen of Caenorhabditis elegans upon restoration of O antigen biosynthesis. *Molecular Microbiology* **87**, 939-950, doi:10.1111/mmi.12144 (2013).
15 Prahathees J. Eswara, K. S. R. Bacterial Cell Division: Nonmodels Poised to Take the Spotlight. *Annual Reviews of Microbiology*, 393-411, doi:10.1146/annurev-micro- (2017).
16 Moore, D. A., Whatley, Z. N., Joshi, C. P., Osawa, M. & Erickson, H. P. Probing for Binding Regions of the FtsZ Protein Surface through Site-Directed Insertions: Discovery of Fully Functional FtsZ-Fluorescent Proteins. *Journal of Bacteriology* **199**, doi:10.1128/JB.00553-16 (2017).
17 Haeusser, D. P. *et al.* The Kil peptide of bacteriophage lambda blocks Escherichia coli cytokinesis via ZipA-dependent inhibition of FtsZ assembly. *PLoS Genet* **10**, e1004217, doi:10.1371/journal.pgen.1004217 (2014).
18 Szwedziak, P. & Löwe, J. Do the divisome and elongasome share a common evolutionary past? *Current Opinion in Microbiology* **16**, 745-751, doi:10.1016/j.mib.2013.09.003 (2013).
19 Broughton, C. E., Van Den Berg, H. A., Wemyss, A. M., Roper, D. I. & Rodger, A. Beyond the Discovery Void: New Targets for Antibacterial Compounds. *Science Progress* **99**, 153-182, doi:10.3184/003685016X14616130512308 (2016).
20 Dow, C. E., van den Berg, H. A., Roper, D. I. & Rodger, A. Biological Insights from a Simulation Model of the Critical FtsZ Accumulation Required for Prokaryotic Cell Division. *Biochemistry* **54**, 3803-3813, doi:10.1021/acs.biochem.5b00261 (2015).
21 Haydon, D. J. *et al.* An Inhibitor of FtsZ with Potent and Selective Anti-Staphylococcal Activity. *Science* **321**, 1673, doi:10.1126/science.1159961 (2008).
22 Hernandez-Rocamora, V. M., Alfonso, C., Margolin, W., Zorrilla, S. & Rivas, G. Evidence That Bacteriophage lambda Kil Peptide Inhibits Bacterial Cell Division by Disrupting FtsZ Protofilaments and Sequestering Protein Subunits. *J Biol Chem* **290**, 20325-20335, doi:10.1074/jbc.M115.653329 (2015).

23 Kiro, R. *et al.* Gene product 0.4 increases bacteriophage T7 competitiveness by inhibiting host cell division. *Proc Natl Acad Sci U S A* **110**, 19549-19554, doi:10.1073/pnas.1314096110 (2013).
24 Studier, F. W. Bacteriophage T7. *Science* **176**, 367-376, doi:10.1126/science.176.4033.367 (1972).
25 Tripathy, S. & Sahu, S. K. FtsZ inhibitors as a new genera of antibacterial agents. *Bioorg Chem* **91**, 103169, doi:10.1016/j.bioorg.2019.103169 (2019).
26 Moller-Olsen, C. *et al.* Bacteriophage K1F targets Escherichia coli K1 in cerebral endothelial cells and influences the barrier function. *Sci Rep* **10**, 8903, doi:10.1038/s41598-020-65867-4 (2020).
27 Galli, E. & Gerdes, K. Spatial resolution of two bacterial cell division proteins: ZapA recruits ZapB to the inner face of the Z-ring. *Mol Microbiol* **76**, 1514-1526 (2010).
28 Eric R. Vimr, F. A. T. Regulation of Sialic Acid Metabolism in Escherichia coli: Role of NAcylneuraminate Pyruvate-Lyase. *The Journal of Bacteriology* **164**, 854-860 (1985).
29 Moller-Olsen, C., Ho, S. F. S., Shukla, R. D., Feher, T. & Sagona, A. P. Engineered K1F bacteriophages kill intracellular Escherichia coli K1 in human epithelial cells. *Sci Rep* **8**, 17559, doi:10.1038/s41598-018-35859-6 (2018).
30 Moore, D. A., Whatley, Z. N., Joshi, C. P., Osawa, M. & Erickson, H. P. Probing for Binding Regions of the FtsZ Protein Surface through Site-Directed Insertions: Discovery of Fully Functional FtsZ-Fluorescent Proteins. *J Bacteriol* **199**, doi:10.1128/JB.00553-16 (2017).
31 Baba, T. *et al.* Construction of Escherichia coli K-12 in-frame, single-gene knockout mutants: the Keio collection. *Mol Syst Biol* **2**, 2006.0008, doi:10.1038/msb4100050 (2006).
32 Studier, F. W. The genetics and physiology of bacteriophage T7. *Virology* **39**, 562-574 (1969).
33 Shaner, N. C. *et al.* Improved monomeric red, orange and yellow fluorescent proteins derived from Discosoma sp. red fluorescent protein. *Nature Biotechnology* **22**, 1567-1572, doi:10.1038/nbt1037 (2004).
34 Meier, C., Oelschlaeger, T. A., Merkert, H., Korhonen, T. K. & Hacker, J. Ability of Escherichia coli isolates that cause meningitis in newborns to invade epithelial and endothelial cells. *Infect Immun* **64**, 2391-2399, doi:10.1128/iai.64.7.2391-2399.1996 (1996).
35 Sahu, U. & Kar, S. Outsider to insider: resetting the natural host niche of commensal E. coli K12. *Bioeng Bugs* **3**, 133-137, doi:10.4161/bbug.19686 (2012).
36 Tak Mak, M. S., Bradley Jett. in *Immunity to Infection* 295–332 (2014).
37 Śliwka, P., Ochocka, M. & Skaradzińska, A. Applications of bacteriophages against intracellular bacteria. *Crit Rev Microbiol* **48**, 222-239, doi:10.1080/1040841x.2021.1960481 (2022).
38 Shan, J. *et al.* Bacteriophages are more virulent to bacteria with human cells than they are in bacterial culture; insights from HT-29 cells. *Sci Rep* **8**, 5091, doi:10.1038/s41598-018-23418-y (2018).
39 Chen, Y., Huang, H., Osawa, M. & Erickson, H. P. ZipA and FtsA* stabilize FtsZ-GDP miniring structures. *Scientific Reports* **7**, 3650, doi:10.1038/s41598-017-03983-4 (2017).
40 Molshanski-Mor, S. *et al.* Revealing bacterial targets of growth inhibitors encoded by bacteriophage T7. *Proc Natl Acad Sci U S A* **111**, 18715-18720, doi:10.1073/pnas.1413271112 (2014).
41 Cahill, J. & Young, R. Phage Lysis: Multiple Genes for Multiple Barriers. *Adv Virus Res* **103**, 3370, doi:10.1016/bs.aivir.2018.09.003 (2019).
42 Shen, B. & Lutkenhaus, J. Differences in MinC/MinD sensitivity between polar and internal Z rings in Escherichia coli. *Journal of bacteriology* **193**, 367-376, doi:10.1128/JB.01095-10 (2011).
43 Hu, Z., Mukherjee, A., Pichoff, S. & Lutkenhaus, J. The MinC component of the division site selection system in Escherichia coli interacts with FtsZ to prevent polymerization. *Proceedings of the National Academy of Sciences* **96**, 14819, doi:10.1073/pnas.96.26.14819 (1999).

Main text figure legends

Table 1: Bacterial strains used in this study

Table 2: Phage strains used in this study

Figure 1: Visualisation of the FtsZ Z-ring in normal growth conditions by confocal microscopy. (A) K12/FtsZ-mNeon cells fixed during human cell infection. An internalisation experiment using gentamicin to kill extracellular bacteria showed this strain had an infection rate of 4.1% in hCMECs. **(B)** EV36/FtsZ-mCherry cells fixed during human cell infection. Arrows pointing to bacterial Z-rings. DAPI stain is shown in blue, phalloidin stain is shown in grey, FtsZ-mNeon is shown in green and FtsZ-mCherry is shown in red.

Figure 2: Visualising bacteriophage in hCMEC brain cells. **(A)** K1F-GFP phage inside vacuole of hCMEC cell after infection. **(B)** T7-mCherry phage inside hCMEC cells after infection. Arrows pointing to phage clusters. DAPI stain is shown in blue, phalloidin stain is shown in grey, K1F-GFP is shown in green and T7-mCherry is shown in red.

Figure 3: T7 phage inhibition of FtsZ in K12 *E. coli* cells. (A-B) Fluorescent images of K12/FtsZ-mNeon cells after T7-mCherry phage infection fixed in a human cell model. Arrows point to filamentous cells. DAPI stain is shown in blue, phalloidin in grey and FtsZ-mNeon in green. **(C-D)** Quantification of Z ring number and cell length for 75 K12/FtsZ-mNeon bacterial cells infected with T7-mCherry phage at 15 minute intervals and compared to a no-phage control. Averages plotted with error bars showing one standard deviation of uncertainty. (E) Quantification of cell length for 75 K12 control and K12ΔminC bacterial cells. Tukey's tests were performed and the calculated probability values (p-values) are displayed as $p < 0.01$ (**).

Figure 4: K1F phage inhibition of FtsZ in K1 *E. coli*. (A-B) Fluorescent images of EV36/FtsZ-mCherry cells after K1F-GFP phage infection fixed in a human cell model. Arrows point to filamentous cells. DAPI stain is shown in blue, phalloidin in grey and FtsZ-mCherry in red. **(C-D)** Quantification of Z ring number and cell length for 75 EV36/FtsZ-mCherry bacterial cells infected with K1F-GFP phage and compared to a no-phage control. Averages plotted with error bars showing one standard deviation of uncertainty. Tukey's tests were performed and the calculated probability values (p-values) are displayed as $p < 0.05$ (*), $p < 0.01$ (**), and not statistically significant $p > 0.05$ (ns).

Figure 5: Effects of T7 bacteriophage on ZapA and FtsI divisome proteins (A) Light microscopy images of K12 control and K12ΔzapA cells after T7 phage infection. **(B)** Quantification of cell length for 75 K12 control and K12ΔzapA bacterial cells infected with T7 phage and compared to a no-phage control. Averages plotted with error bars showing one standard deviation of uncertainty. Tukey's tests were performed and the calculated probability values (p-values) are displayed as $p < 0.05$ (*), $p < 0.01$ (**) and not statistically significant $p > 0.05$ (ns). **(C)** *E. coli* K12 cell stained with an FtsI antibody showing localisation of FtsI to the cell midbody as a single ring. **(D)** *E. coli* K12 cell after T7 phage infection stained with an FtsI antibody showing mislocalisation of FtsI to three rings.

Figure 6: T7Δ0.4 mutant phage microscopy. (A) K12/FtsZ-mNeon control cells fixed in human cells. **(B)** K12/FtsZ-mNeon cells infected with T7-mCherry phage fixed in human cells. **(C)** K12/FtsZ-mNeon cells infected with T7Δ0.4 phage fixed in human cells. For fluorescent images DAPI stain is shown in blue, phalloidin in grey and FtsZ-mNeon in green. Arrows pointing to bacterial cell of interest. **(D-E)** Quantification of Z ring number and cell length for 75 K12/FtsZ-mNeon bacterial cells infected with T7-mCherry or T7Δ0.4 phage during exponential growth and compared to a no-phage control. Averages plotted with error bars showing one standard deviation of uncertainty. Tukey's tests were performed and the calculated probability values (p-values) are displayed as $p < 0.05$ (*), $p < 0.01$ (**), and not statistically significant $p > 0.05$ (ns).

Figure 7: T7Δ0.4 mutant experiments showing gp0.4 delays lysis and increases progeny. (A) WT T7 and T7Δ0.4 phages were propagated and titred by plaque assays in triplicate. Averages plotted on a log scale with

error bars showing one standard deviation of uncertainty. **(B)** Growth curves were performed on cultures of K12/FtsZ-mNeon only, K12/FtsZ-mNeon and WT T7, K12/FtsZ-mNeon and T7Δ0.4 phage. Average readings across replicates at 15 minute time intervals were plotted with error bars showing one standard deviation unit of uncertainty. Arrow shows when phage was added. **(C)** Photo time series of growth curves with images of cultures taken upon phage addition at 75 minutes, at 120 minutes showing T7Δ0.4 lysis, and 180 minutes showing WT T7 lysis.

Figure 8: Stationary phase microscopy quantification of WT T7 and T7Δ0.4 infection. Quantification of **(A)** Z ring number and **(B)** cell length for 75 K12/FtsZ-mNeon bacterial cells infected with T7mCherry or T7Δ0.4 phage during the stationary phase of growth, along with a no-phage control, compared to exponential phase data. Tukey's tests were performed and the calculated probability values (p-values) are displayed as $p < 0.05$ (*), $p < 0.01$ (**), and not statistically significant $p > 0.05$ (ns). **(C)** Exponential phase control, stationary phase control, exponential phase with T7 phage and stationary phase with T7 phage cultures of *E. coli* K12/FtsZ-mNeon were imaged on agarose pads, and the corrected total cell fluorescence (CTCF) of 50 Z-rings per sample was averaged and plotted. Error bars show one standard deviation of uncertainty.

Supplementary figure legends

Table S1: Primers. Primers used in the engineering of T7-mCherry phage

Table S2: Table of titres from plaque assays for WT and T7 mutant phages

Figure S1: gBlock insert designed to make fluorescent T7 phage. A gBlock was designed to create a recombinant T7-mCherry phage. The BioBrick regions at the ends shown in blue contain restriction sites to allow cloning into a vector. Homology regions shown in pink contain 150 bp of DNA before and after the stop codon of the minor capsid protein. The mCherry gene is shown in red and the linker region is shown in green.

Figure S2: Visualisation of the FtsZ Z-ring in normal growth conditions by confocal microscopy. (A) Fluorescent images showing live K12/FtsZ-mNeon cells on agarose pads. **(B)** Live EV36/FtsZ-mCherry cells on agarose pads. FtsZ-mNeon is shown in green and FtsZ-mCherry is shown in red.

Figure S3: Human cell death by extracellular bacterial strains. HCMEC human brain cells were infected with the K12/FtsZ-mNeon and EV36/FtsZ-mCherry strains live, along with a no bacteria control, and numbers of dying human cells were counted and the percentage cell death was quantified as follows: 4.8% hCMEC cell death in control conditions, 5.3% hCMEC cell death following K12 infection, and 12.1% hCMEC cell death following EV36 infection. Cell outlines are shown by transmitted light and DAPI stain was used to show DNA in blue. Arrows are pointing to dying human cells. For each condition the experiments were repeated in triplicate and a minimum of 500 human cells per condition were counted.

Figure S4: Kil peptide inhibition of *E. coli* FtsZ. **(A)** Different phenotypes of K12/FtsZ-mNeon/Kil. Left image shows multiple distinct Z-rings, right images shows diffuse spread and middle images shows an intermediate phenotype. **(B)** K12/FtsZ-mNeon/Kil cell fixed in human cell infection. Arrow pointing to filamentous bacterial cells. Images taken one 2 hours after plasmid induction. DAPI stain is shown in blue, phalloidin stain is shown in grey and FtsZ-mNeon is shown in green. **(C-D)** Quantification of Z ring number and cell length for 75 K12/FtsZ-mNeon/Kil bacterial cells under the following conditions: control, 1 hour plasmid induction, 2 hour plasmid induction. Mean averages plotted with error bars showing one standard deviation of uncertainty. Tukey's tests were performed and the calculated probability values (p-values) are displayed as $p < 0.05$ (*), $p < 0.01$ (**), and not statistically significant $p > 0.05$ (ns).

Figure S5: Kil inhibition of E. coli EV36 FtsZ. EV36/Kil cell fixed in human cell infection with anti-Prokaryotic Cell Division GTPase (FtsZ) antibody staining**. (A)** Control with no Kil induction **(B)** Elongated cell after Kil induction

Figure S6: Screening for recombinant phage after homologous recombination
(A) Phage culture screening round 1 PCR after homologous recombination
(B and C) Plaque assay of positive culture and screening of individual plaques
(D) Positive plaques propagated and further PCR test on liquid culture
(E) CsCl purification band of positive T7-mCherry culture
(F) Plaque assay to titre the recombinant phage

Figure S7: No-phage controls for experiments visualising phages in human cells. **(A-B)** No phage control samples for visualisation of K1F-GFP phage in hCMEC, showing no contamination or background fluorescence inside the human cells**. (C-D)** No phage control samples for visualisation of T7-mCherry phage in hCMEC, showing no contamination or background fluorescence inside the human cells. DAPI stain is shown in blue, phalloidin in grey, K1F-GFP in green and T7-mCherry in red

Figure S8: Growth curves. **(A)** Growth curves for EV36, EV36/FtsZ-mCherry and EV36/FtsZ-mCherry with K1F-GFP phage. OD600 readings were taken every 30 minutes and phage was added after OD600 passed 0.3 at 90 minutes **(B)** Growth curves for MG1655, K12/FtsZ-mNeon and K12/FtsZ-mNeon with T7 phage. OD600 readings taken every 30 minutes and phage was added after OD600 passed 0.3 at 90 minutes.

Figure S9: Correlative light and electron microscopy. Correlative light and electron microscopy (CLEM) images of *E. coli* K12/FtsZ-mNeon after 60 minutes of T7 infection. Left panel shows EM image, middle shows confocal T7-mCherry channel and right shows confocal mNeon channel.

Figure S10. Control (no phage) time series of K12/FtsZ-mNeon in hCMEC cells. (A) 45 minutes incubation of K12/FtsZ-mNeon **(B)** 60 minutes incubation of K12/FtsZ-mNeon **(C)** 75 minutes incubation of K12/FtsZ-mNeon **(D)** 105 minutes incubation of K12/FtsZ-mNeon **(E)** 120 minutes incubation with FtsZ-mNeon.

Figure S11. Time series of K12/FtsZ-mNeon infected with T7-mCherry in hCMEC cells. (A) 0 minutes incubation of K12/FtsZ-mNeon with T7-mCherry **(B)** 30 minutes incubation of K12/FtsZ-mNeon with T7-mCherry **(C)** 45 minutes incubation of K12/FtsZ-mNeon with T7-mCherry **(D)** 60 minutes incubation of K12/FtsZ-mNeon with T7-mCherry **(E)** 75 minutes incubation of K12/FtsZ-mNeon with T7-mCherry.

Figure S12: Mutated MinC leads to cell filamentation (A) Confocal microscopy image of K12 control cells after FtsZ antibody staining. **(B)** Confocal microscopy image of K12ΔminC cells after FtsZ antibody staining. DAPI stain is shown in blue, phalloidin in grey, and FtsZ in green. Arrows point to cells of interest.

Figure S13: Growth curve showing the effect of bacteriostatic antibiotics on host cell lysis. Growth curves for K12/FtsZ-mNeon with WT T7 phage and T7Δ0.4 phage, alongside a no phage control (solid lines), and curves for K12/FtsZ-mNeon with WT T7 phage and T7Δ0.4 phage, alongside a no phage control with a bacteriostatic concentration of chloramphenicol added to each culture (dashed lines). OD600 readings taken every 5 minutes, and phage and chloramphenicol was added when needed after OD600 passed 0.3 at 90 minutes.

Figure S14: Representative images used for calculated total cell fluorescence (CTCF). Cultures of E. coli K12/FtsZ-mNeon in the exponential phase, K12/FtsZ-mNeon in the stationary phase, K12/ FtsZmNeon and T7 phage in the exponential phase, and K12/ FtsZ-mNeon and T7 phage in the stationary phase were grown and imaged on triplicate agarose pads. 50 cells per condition were quantified for their CTCF using fluorescence intensity measurements calculated on FiJi.

Figure 1.JPEG

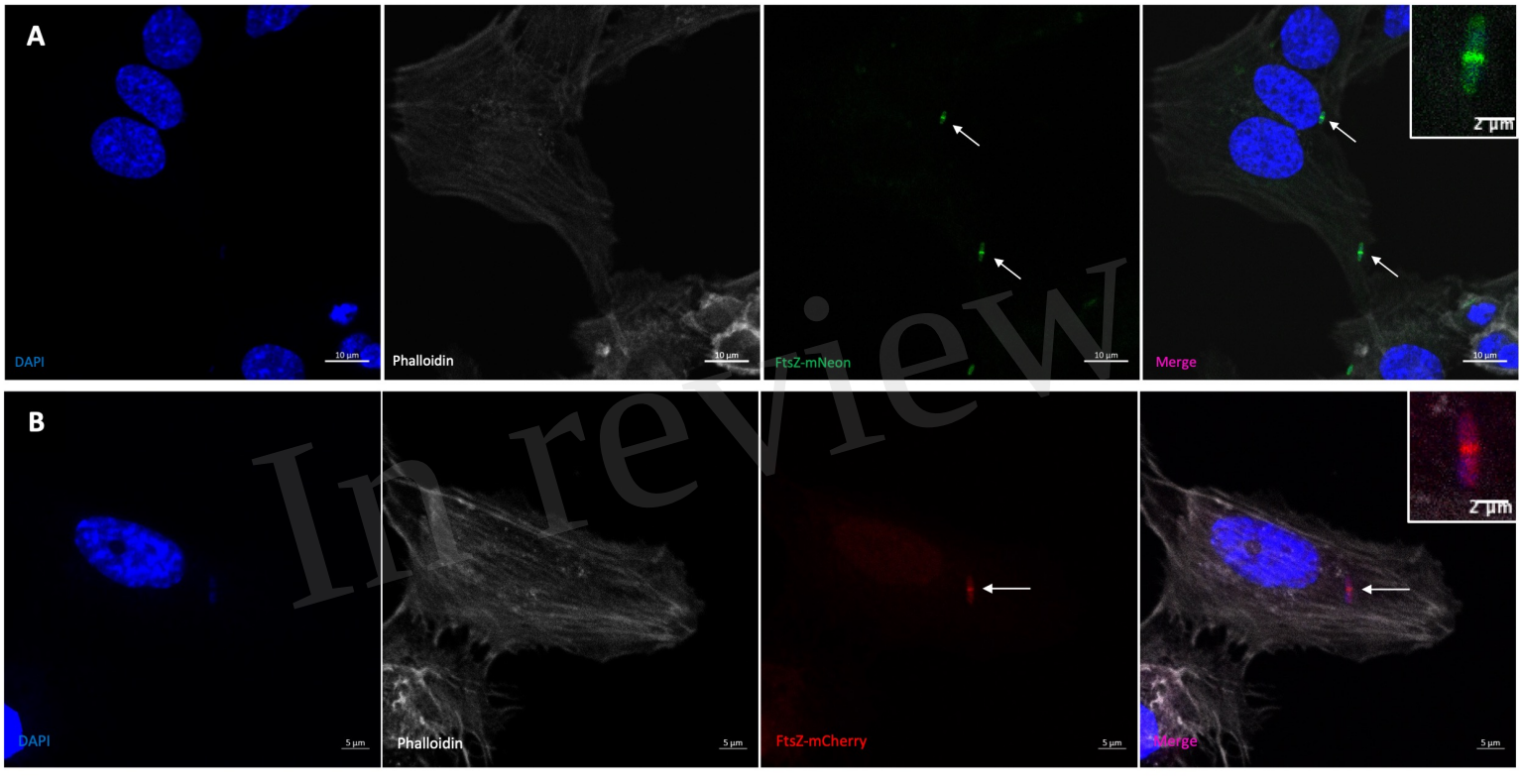

Figure 1: Visualisation of the FtsZ Z-ring in normal growth conditions by confocal microscopy. (A) K12/FtsZ-mNeon cells fixed during human cell infection. An internalisation experiment using gentamicin to kill extracellular bacteria showed this strain had an infection rate of 4.1% in hCMECs. **(B)** EV36/FtsZ-mCherry cells fixed during human cell infection. Arrows pointing to bacterial Z-rings. DAPI stain is shown in blue, phalloidin stain is shown in grey, FtsZ-mNeon is shown in green and FtsZ-mCherry is shown in red.

Figure 2.JPEG

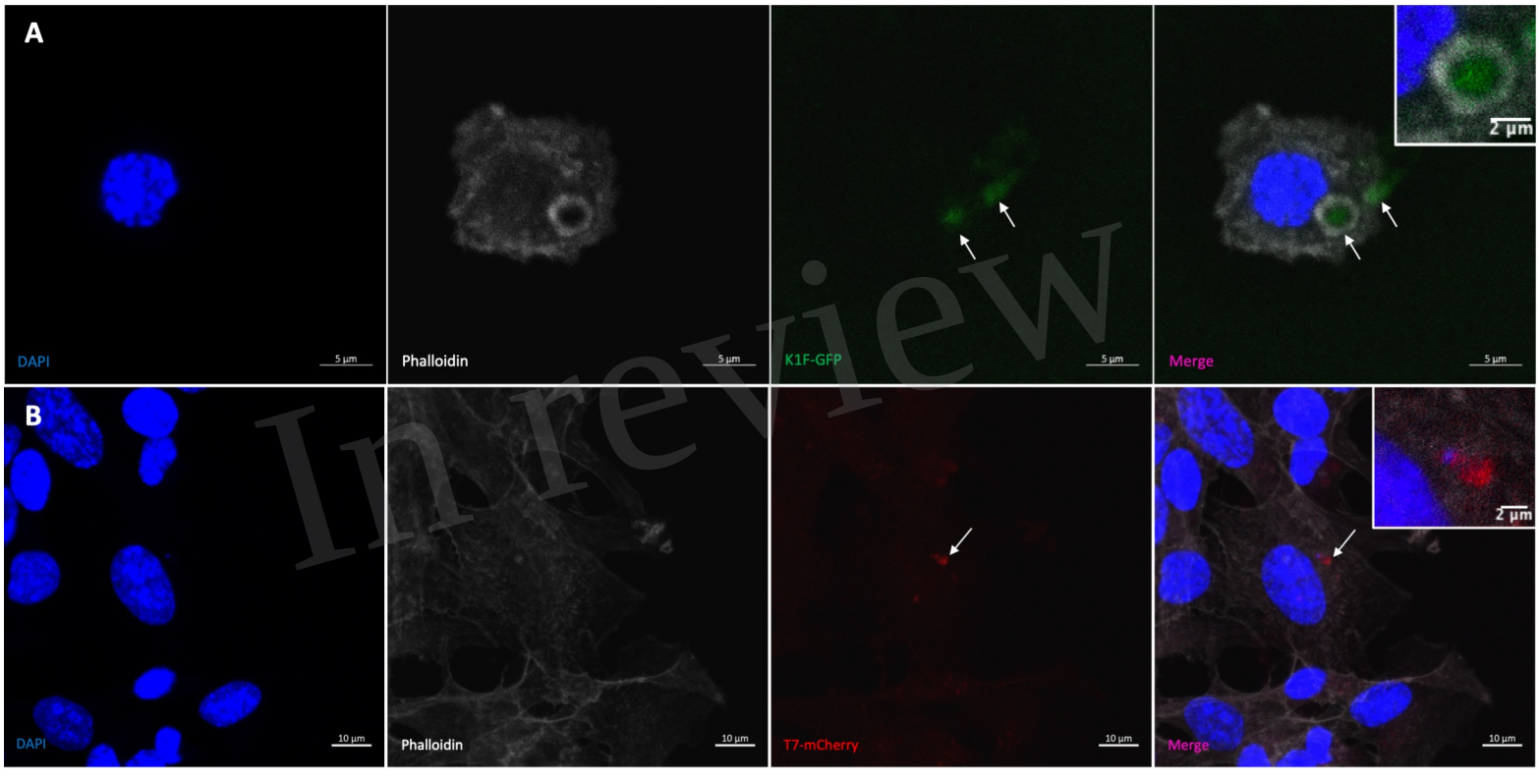

Figure 2: Visualising bacteriophage in hCMEC brain cells. **(A)** K1F-GFP phage inside vacuole of hCMEC cell after infection. **(B)** T7-mCherry phage inside hCMEC cells after infection. Arrows pointing to phage clusters. DAPI stain is shown in blue, phalloidin stain is shown in grey, K1F-GFP is shown in green and T7-mCherry is shown in red.

Figure 3.JPEG

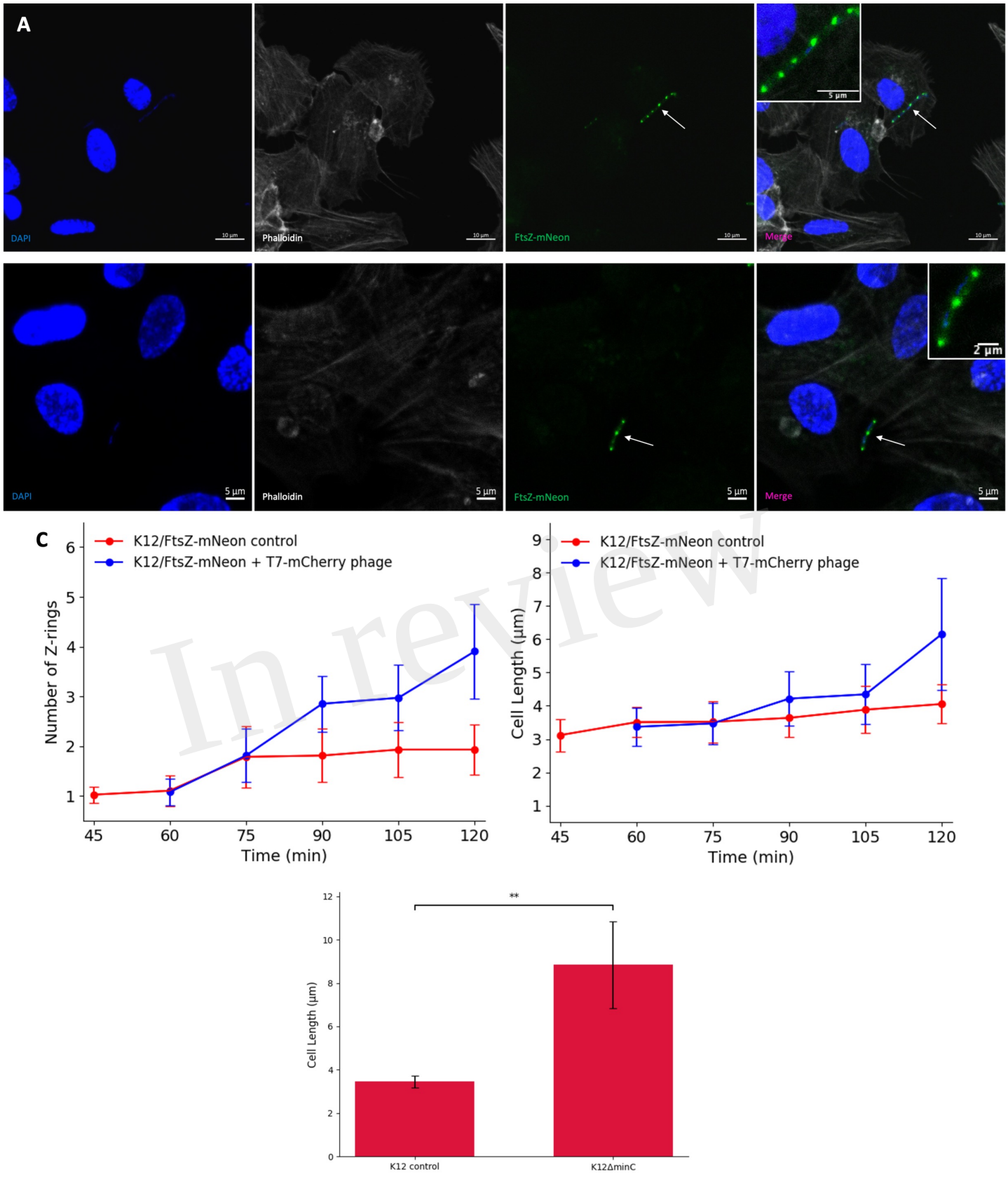

Figure 3: T7 phage inhibition of FtsZ in K12 *E. coli* cells.. (A-B) Fluorescent images of K12/FtsZ-mNeon cells after T7-mCherry phage infection fixed in a human cell model. Arrows point to filamentous cells. DAPI stain is shown in blue, phalloidin in grey and FtsZ-mNeon in green. **(C-D)** Quantification of Z ring number and cell length for 75 K12/FtsZ-mNeon bacterial cells infected with T7-mCherry phage at 15 minute intervals and compared to a no-phage control. Averages plotted with error bars showing one standard deviation of uncertainty. (E) Quantification of cell length for 75 K12 control and K12ΔminC bacterial cells. Tukey's tests were performed and the calculated probability values (p-values) are displayed as $p \leq 0.01$ (**).

Figure 4.JPEG

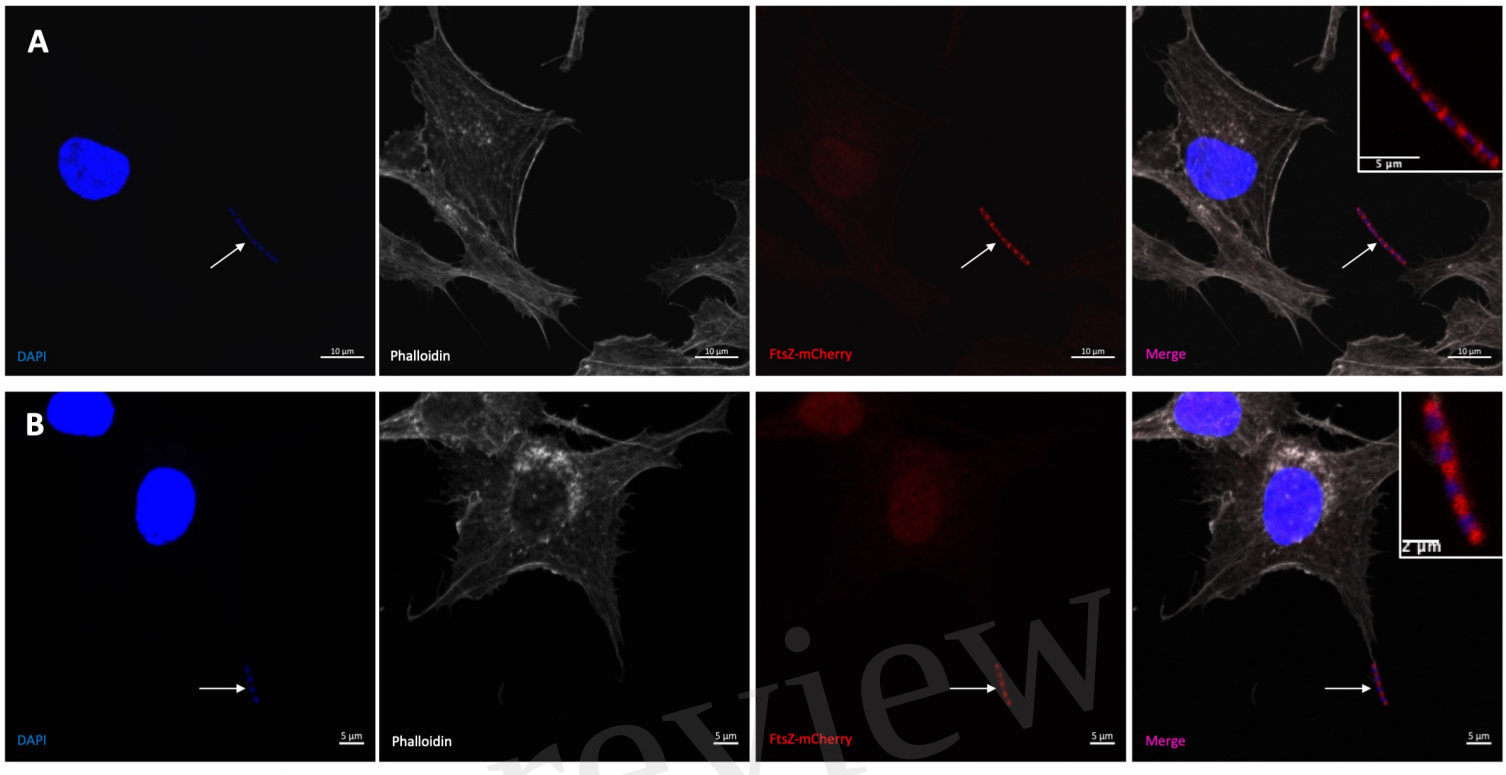

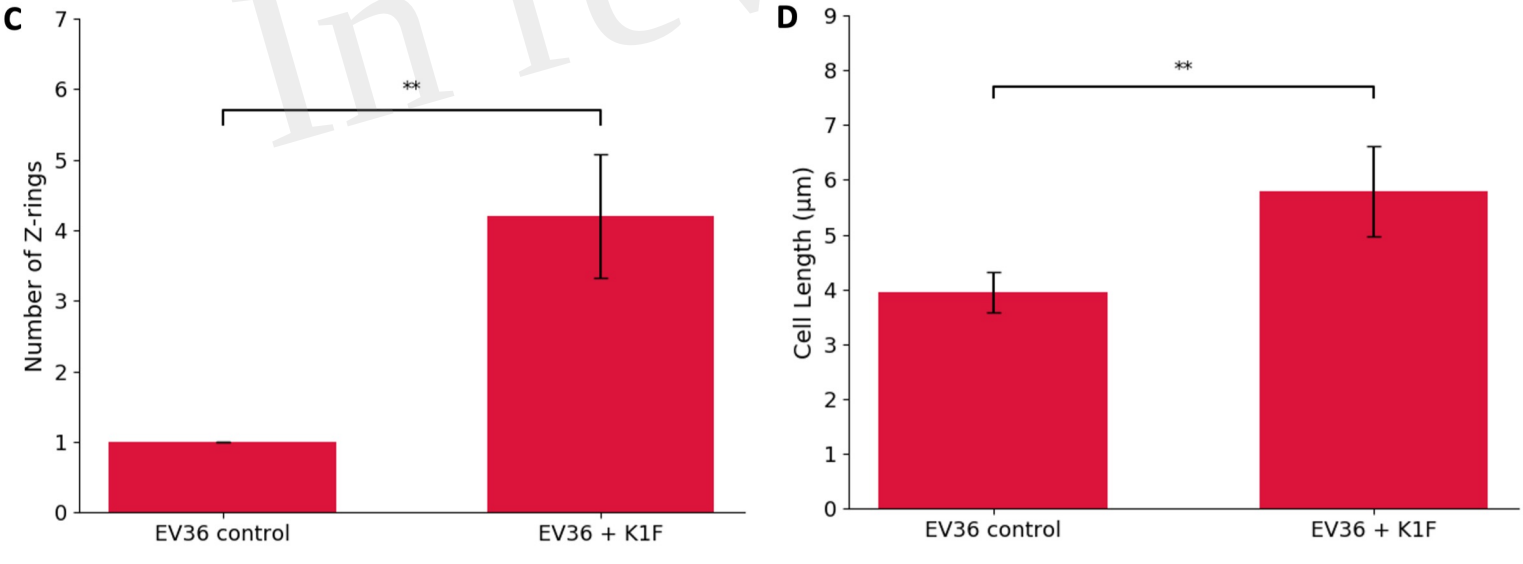

Figure 4: K1F phage inhibition of FtsZ in K1 *E. coli*. (A-B) Fluorescent images of EV36/FtsZ-mCherry cells after K1F-GFP phage infection fixed in a human cell model. Arrows point to filamentous cells. DAPI stain is shown in blue, phalloidin in grey and FtsZ-mCherry in red. **(C-D)** Quantification of Z ring number and cell length for 75 EV36/FtsZ-mCherry bacterial cells infected with K1F-GFP phage and compared to a no-phage control. Averages plotted with error bars showing one standard deviation of uncertainty. Tukey's tests were performed and the calculated probability values (p-values) are displayed as $p \leq 0.05$ (*), $p \leq 0.01$ (**), and not statistically significant $p \geq 0.05$ (ns).

Figure 5.JPEG

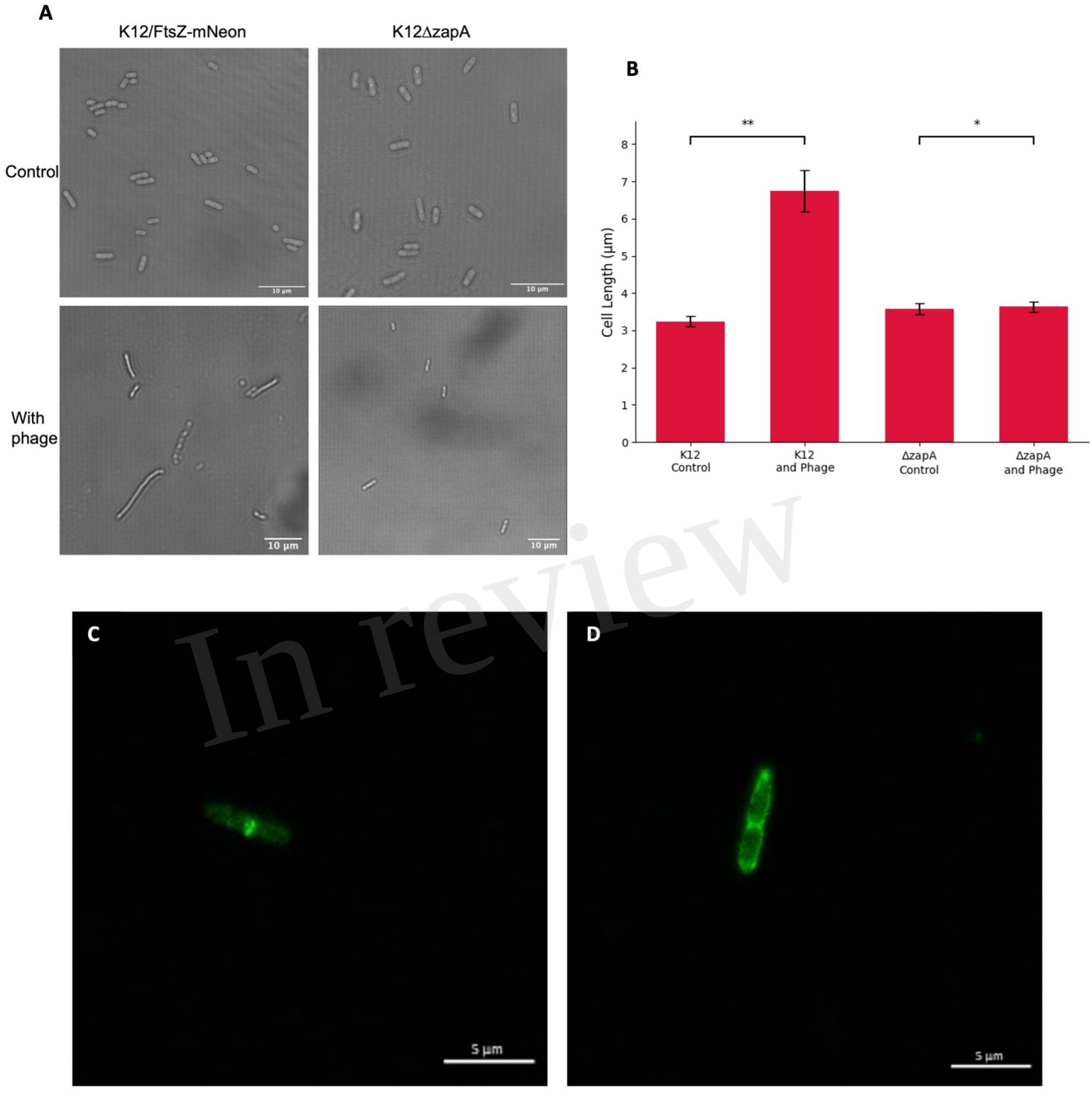

Figure 5: Effects of T7 bacteriophage on ZapA and FtsI divisome proteins (A) Light microscopy images of K12 control and K12ΔzapA cells after T7 phage infection. **(B)** Quantification of cell length for 75 K12 control and K12ΔzapA bacterial cells infected with T7 phage and compared to a no-phage control. Averages plotted with error bars showing one standard deviation of uncertainty. Tukey's tests were performed and the calculated probability values (p-values) are displayed as $p \leq 0.05$ (*), $p \leq 0.01$ (**) and not statistically significant $p \geq 0.05$ (ns). **(C)** *E. coli* K12 cell stained with an FtsI antibody showing localisation of FtsI to the cell midbody as a single ring. **(D)** *E. coli* K12 cell after T7 phage infection stained with an FtsI antibody showing mislocalisation of FtsI to three rings.

Figure 6.JPEG

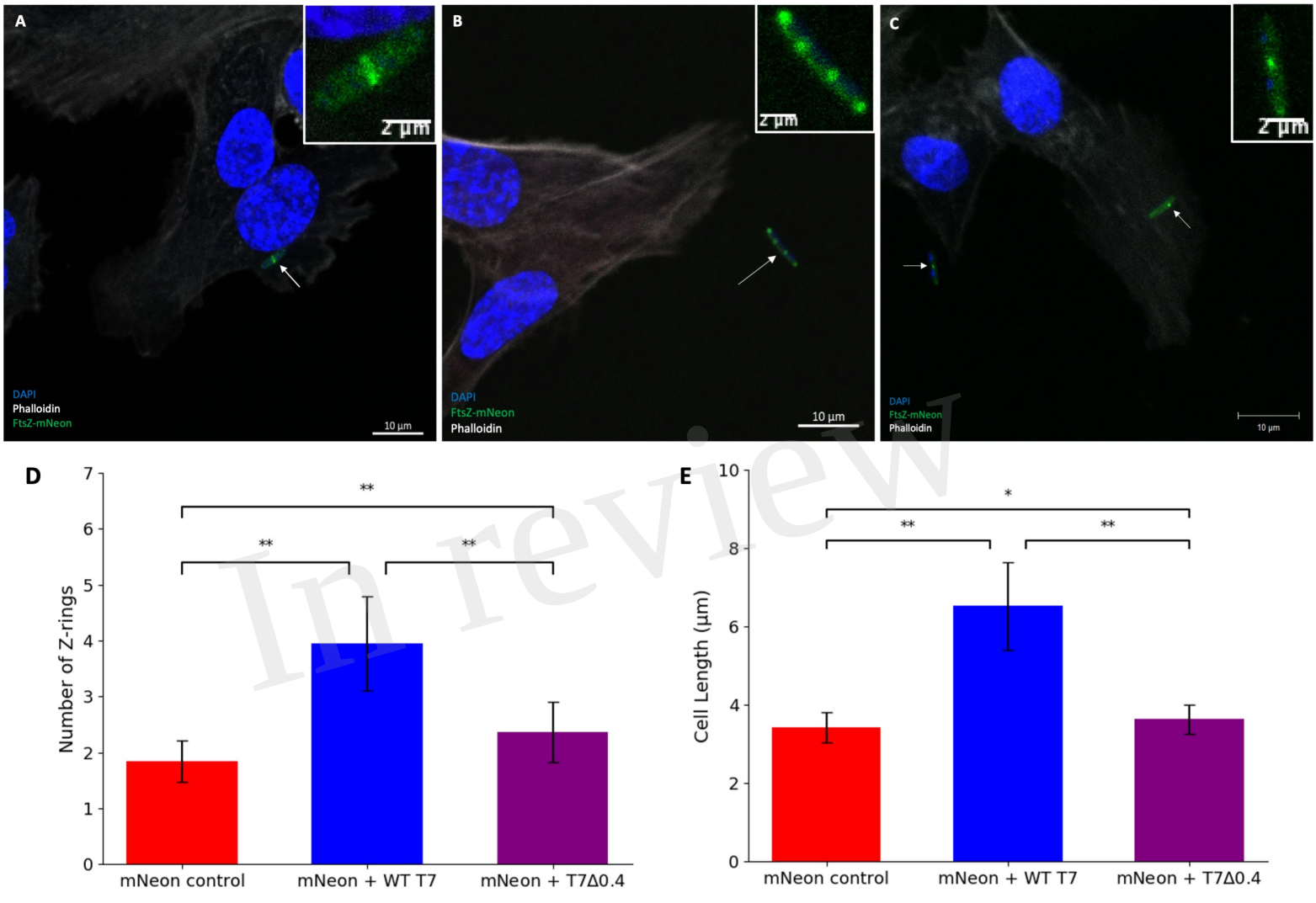

Figure 6: T7Δ0.4 mutant phage microscopy. (A) K12/FtsZ-mNeon control cells fixed in human cells. **(B)** K12/FtsZ-mNeon cells infected with T7-mCherry phage fixed in human cells. **(C)** K12/FtsZ-mNeon cells infected with T7Δ0.4 phage fixed in human cells. For fluorescent images DAPI stain is shown in blue, phalloidin in grey and FtsZ-mNeon in green. Arrows pointing to bacterial cell of interest. **(D-E)** Quantification of Z ring number and cell length for 75 K12/FtsZ-mNeon bacterial cells infected with T7-mCherry or T7Δ0.4 phage during exponential growth and compared to a no-phage control. Averages plotted with error bars showing one standard deviation of uncertainty. Tukey's tests were performed and the calculated probability values (p-values) are displayed as $p \leq 0.05$ (*), $p \leq 0.01$ (**), and not statistically significant $p \geq 0.05$ (ns).

Figure 7.JPEG

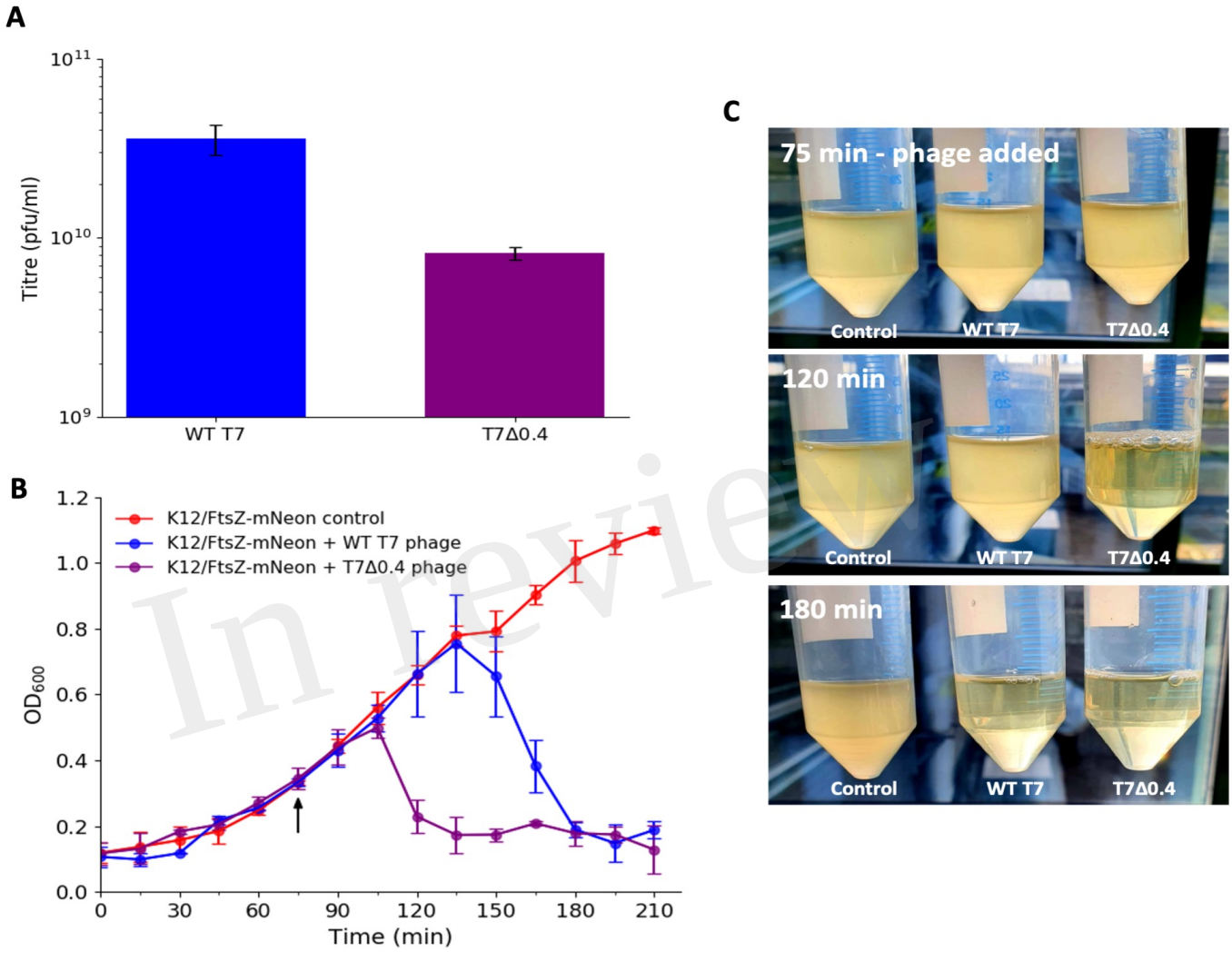

Figure 7: T7Δ0.4 mutant experiments showing gp0.4 delays lysis and increases progeny. (A) WT T7 and T7Δ0.4 phages were propagated and titred by plaque assays in triplicate. Averages plotted on a log scale with error bars showing one standard deviation of uncertainty. **(B)** Growth curves were performed on cultures of K12/FtsZ-mNeon only, K12/FtsZ-mNeon and WT T7, K12/FtsZ-mNeon and T7Δ0.4 phage. Average readings across replicates at 15 min time intervals were plotted with error bars showing one standard deviation unit of uncertainty. Arrow shows when phage was added. **(C)** Photo time series of growth curves with images of cultures taken upon phage addition at 75 minutes, at 120 minutes showing T7Δ0.4 lysis, and 180 minutes showing WT T7 lysis.

Figure 8.JPEG

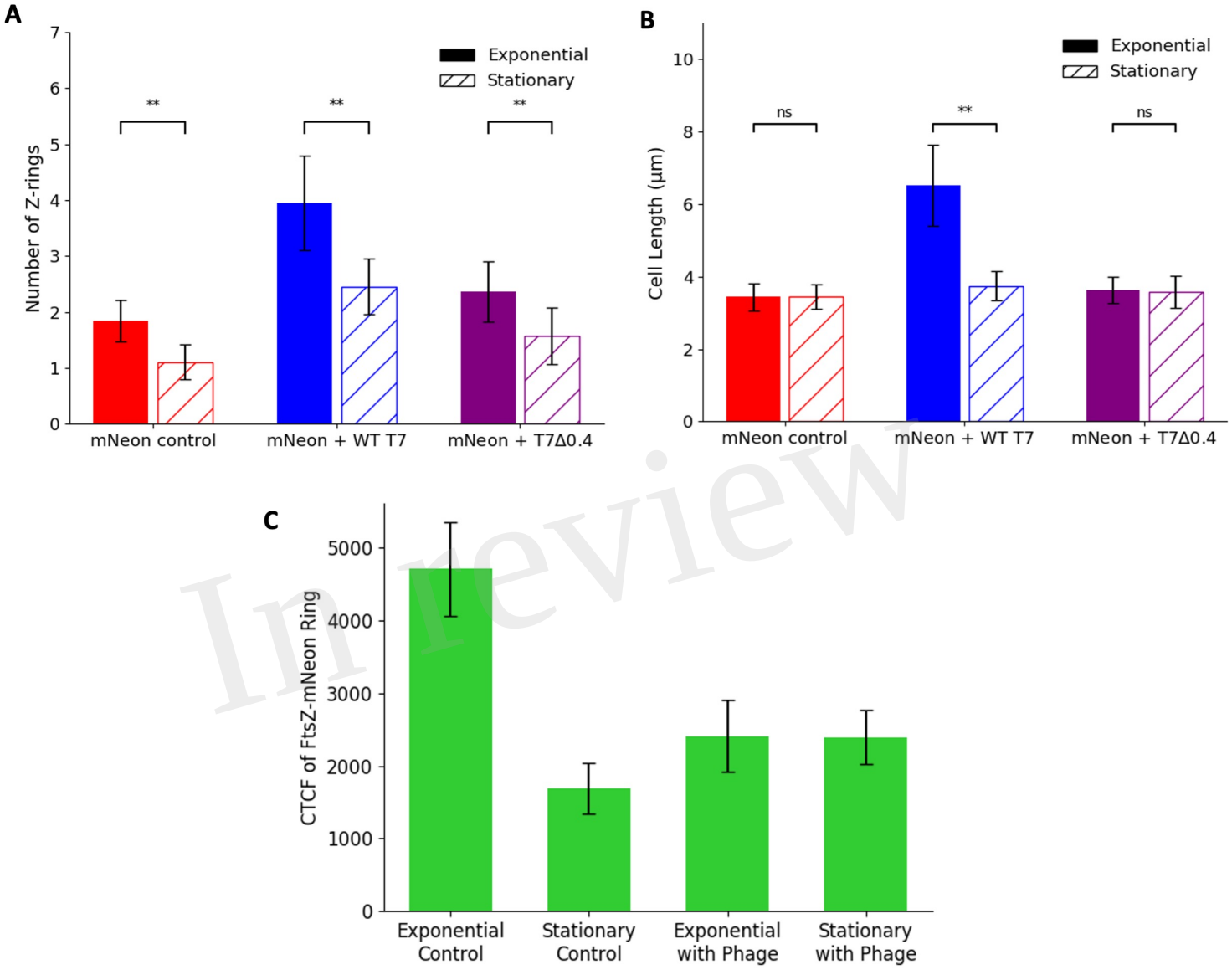

Figure 8: Stationary phase microscopy quantification of WT T7 and T7Δ0.4 infection. Quantification of **(A)** Z ring number and **(B)** cell length for 75 K12/FtsZ-mNeon bacterial cells infected with T7-mCherry or T7Δ0.4 phage during the stationary phase of growth, along with a no-phage control, compared to exponential phase data. Tukey's tests were performed and the calculated probability values (p-values) are displayed as $p \leq 0.05$ (*), $p \leq 0.01$ (**), and not statistically significant $p \geq 0.05$ (ns). **(C)** Exponential phase control, stationary phase control, exponential phase with T7 phage and stationary phase with T7 phage cultures of *E. coli* K12/FtsZ-mNeon were imaged on agarose pads, and the corrected total cell fluorescence (CTCF) of 50 Z-rings per sample was averaged and plotted. Error bars show one standard deviation of uncertainty.